NASA
SPACE VEHICLE
DESIGN CRITERIA
(GUIDANCE AND CONTROL)

NASA SP-8078

SPACEBORNE ELECTRONIC IMAGING SYSTEMS

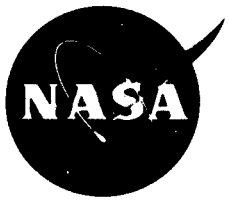

JUNE 1971

NATIONAL AERONAUTICS AND SPACE ADMINISTRATION

GUIDE TO THE USE OF THIS MONOGRAPH

The purpose of this monograph is to organize and present, for effective use in spacecraft development, the significant experience and knowledge accumulated in development and operational programs to date. It reviews and assesses current design practices, and from them establishes firm guidance for achieving greater consistency in design, increased reliability in the end product, and greater efficiency in the design effort. The monograph is organized into three major sections that are preceded by a brief *Introduction* and complemented by a set of *References.*

The *State of the Art,* section 2, reviews and discusses the total design problem, and identifies *which* design elements are involved in successful designs. It describes succinctly the current technology pertaining to these elements. When detailed information is required, the best available references are cited. This section serves as a survey of the subject that provides background material and prepares a proper technological base for the *Design Criteria* and *Recommended Practices.*

The *Design Criteria,* shown in section 3, state clearly and briefly what rule, guide, limitation, or standard must be imposed on each essential design element to insure successful design. The *Design Criteria* can serve effectively as a checklist for the project manager to use in guiding a design or in assessing its adequacy.

The *Recommended Practices,* as shown in section 4, state how to satisfy each of the criteria. Whenever possible, the best procedure is described; when this cannot be done concisely, appropriate references are provided. The *Recommended Practices,* in conjunction with the *Design Criteria,* provide positive guidance to the practicing designer on how to achieve successful design.

The design criteria monograph is not intended to be a design handbook, a set of specifications, or a design manual. It is a summary and a systematic ordering of the large and loosely organized body of existing successful design techniques and practices. Its value and its merit should be judged on how effectively it makes that material available to and useful to the user.

FOREWORD

NASA experience has indicated a need for uniform design criteria for space vehicles. Accordingly, criteria are being developed in the following areas of technology:

Environment
Structures
Guidance and control
Chemical propulsion

Individual monographs of the series will be issued as separate documents as soon as each is completed on a particular subject. This document, *Spaceborne Electronic Imaging Systems,* is one monograph of the Guidance and Control series.

A list of all previously issued monographs can be found at the back of this publication.

The monographs are to be regarded as guides to design and not as NASA requirements except as may be invoked in formal project specifications. It is expected, however, that the criteria presented in these documents, to be revised as experience may indicate to be desirable, eventually may be uniformly applied to the design of NASA space vehicles.

This monograph was prepared under the cognizance of the NASA Electronics Research Center and published by the Jet Propulsion Laboratory. Dr. J. E. Keigler of RCA Astro-Electronics Division was the committee chairman and program manager. Contributions in the areas of design experience and development practices were provided by an advisory panel consisting of the following individuals:

J. O. Hamby	Westinghouse Aerospace Division
Donald T. Heckel	Sylvania Electronic Systems
Robert F. Hummer	Santa Barbara Research Center
Edward W. Koenig	ITT Aerospace Optical Division
Max H. Mesner	RCA Astro-Electronics Division
Harvey Ostrow	NASA, Goddard Space Flight Center
Melvin I. Smokler	Jet Propulsion Laboratory
Harold Yates	ESSA National Environment Satellite Center

The effort was guided by:

Jan Bebris	NASA, Electronics Research Center
Raymond F. Bohling	NASA Headquarters
Frank Carroll	NASA, Electronics Research Center

Comments concerning the technical content of this monograph will be welcomed by the National Aeronautics and Space Administration, Office of Advanced Research and Technology (Code RE), Washington, D. C. 20546.

June 1971

CONTENTS

SPACEBORNE ELECTRONIC IMAGING SYSTEMS

1. INTRODUCTION

Electronic imaging systems perform a variety of functions in space vehicles, including the recording of earth cloud patterns and temperature distributions, the recording of surface and atmospheric characteristics of the planets and the moon, and the monitoring of rocket propellants, booms, and crew activities. This monograph provides criteria and recommended practices for the design of the spaceborne elements of these systems.

For the purposes of this monograph, a spaceborne electronic imaging system is defined as a device that collects energy in some portion of the electromagnetic spectrum with detector(s) whose direct output is an electrical signal that can be processed (using direct transmission or delayed transmission after recording) to form a pictorial image. This definition encompasses both image tube systems and scanning point-detector systems, but excludes those in which photographic film is utilized instead of an electrical detector. (Lunar Orbiter is the only such unclassified use of on-board film development with flying spot scanner generation of a video signal for transmission; ref. 1.) The scope of the monograph is thus quite broad, but the intent is not to stress the design details of the many hardware end-items—it is rather to collect the design experience and recommended practice of the several systems possessing the common denominator of acquiring images from space electronically and to maintain the system viewpoint rather than pursuing specialization in devices. The devices may be markedly different physically, but each was designed to provide a particular type of image within particular limitations. Performance parameters which determine the type of system selected for a given mission and which influence the design include:

- Sensitivity
- Resolution
- Dynamic range
- Spectral response
- Frame rate/bandwidth
- Optics compatibility
- Image motion
- Radiation resistance
- Size, weight, power
- Reliability, life

The design of a spaceborne imaging system must provide, within the limits of physical reliability and economic reality, an image of the scene, in spectral regions of interest, with specified fidelity and quality. The design must be compatible with the conditions specified for use, with the physical environment, and with the system interfaces for transmission and recording.

Failure of a design of an imaging system to achieve desired performance, expected life, or space compatibility will often entail failure of the mission even though the remainder of the spacecraft functions perfectly.

2. STATE OF THE ART

The application of spaceborne electronic imaging systems to provide pictorial data from a space vehicle is now in its second decade, and the capabilities of the devices and their varieties of implementation are typical of the technological progress of the decade. While ruggedized adaptations of commercial television cameras were carried on a few early ballistic flights into space, spaceborne electronic imaging came of age when systems were specifically designed for their particular mission applications. An overriding aspect of those early mission applications on unmanned space vehicles was the severe limitation on size, weight, and power, the latter in turn limiting the video transmission bandwidth. Hence so-called slow-scan television evolved, wherein single, shuttered exposures were scanned at a frame rate commensurate with the available bandwidth.

Two other aspects of the mission applications had major influence on the new technology of spaceborne electronic imaging: first, the spacecraft motion could provide one dimension of the image scan, and second, images in spectral regions beyond the visible were necessary. The first led to several variations of line-scan sytems, of both electrically and mechanically scanned types; the second led to far-infrared and multispectral imaging systems that fulfill particular requirements. Finally, of course, with the greater payload capability of manned spacecraft and larger unmanned spacecraft, there have appeared electronic imaging systems more closely paralleling conventional television techniques, including color and very-high-resolution systems.

The types of spaceborne electronic imaging systems can be classified by the four characteristics given in table I.

Table I.—Electronic Imaging System Characteristics

Characteristics	Application
Spectral response	Visible[a] or infrared
Scanning method	Electronic or mechanical
Sensor device	Image tube or point detector(s)
Image format	Frame or line scan

[a]Including near UV and near IR.

Imaging systems comprising the present state of the art correspond to five combinations of these four characteristics as shown in table II.

Table II.—Types of Electronic Imaging Systems

Characteristics	Type I	Type II	Type III	Type IV	Type V
Spectral response	Visible				IR
Scanning method	Electronic			Mechanical	
Sensor device	Tube		Point detector(s)		
Image format	Frame	Line			

Type I is the conventional image-tube frame camera such as those of TIROS (table III), while, at the opposite range of the chart, Type V is the mechanical line scanner such as the Nimbus high-resolution infrared radiometer (HRIR) (table IV). Type IV is then the visible counterpart of Type V, or the visible channel of a dual-channel scanner such as the Improved TIROS Operations System (ITOS) scanning radiometer. Types II and III are typified by the line-scan image dissector and linear solid-state array, respectively. Section 2.1 contains a summary of the operating parameters of all of the electronic imaging systems which have operated in space or are in advanced stages of development for designated spacecraft. The remaining paragraphs of section 2 describe the capabilities and limitations of these systems.

2.1 Review of Design and Flight Experience

The spaceborne electronic imaging systems summarized in tables III and IV represent all of the unclassified imaging systems developed by the United States that have performed in orbit or have progressed past the prototype stage of development. These prerequisites for listing systems under "State of the Art" (section 2) as of the date of this monograph unfortunately exclude the Type III line-scan solid-state arrays which are becoming feasible with advancements in the technology of large-scale integrated circuitry. NASA is funding the development of such arrays for solid-state cameras, however, and the properties of these detectors are included in section 2.3.2.

2.2 Image-Tube Frame Cameras

As shown in the preceding table, cameras have been designed to exploit the capabilities of various types of image tubes for particular missions. Such capabilities include long image retention to permit slow scan for narrow bandwidth applications and high sensitivity for low light levels, so that even within the Type I category (table I), there is a wide range of capabilities and limitations (refs. 33 and 34). By virtue of simultaneous exposure of the entire image surface in a framing mode of operation, the Type I imaging systems are used where a snapshot image is more desirable than the panoramic line-by-line exposure of the line-scan systems or where integration of the image irradiance is necessary for the desired sensitivity.

Table III.—Image Tube Cameras

	Spacecraft	First launch date	Orbit	Application	Sensor	Horizontal resolution (TV lines)	Frame time, sec	Video bandwidth, kHz
TIROS	TIROX I-IX	4-1-60	550 km (300 nmi) inclined	Visible cloud cover	1.27-cm (½-in.) vidicon EM defl and foc	400	2.0	62.5
AVCS	Nimbus	8-28-64	1,110 km (600 nmi) sun-synchronous (noon)	Visible cloud cover	2.54-cm (1-in.) vidicon EM defl and foc	800	6.5	60.0
	TOS/ESSA		1,390 km (750 nmi) sun-synchronous (3 pm)					
	ITOS		1,460 km (790 nmi) sun-synchronous (3 pm)					
	Applications Technology Satellite (ATS)		11,120 km (6000 nmi) equatorial					
APT	TIROS	12-21-63	740 km (400 nmi) inclined	Visible cloud cover	2.54-cm (1-in.) storage vidicon EM defl and foc	700	200	1.6
	Nimbus	8-28-64	1,1100 km (600 nmi) sun-synchronous (noon)					
	TOS/ESSA	2-28-66	1,390 km (750 nmi) sun-synchronous (3 pm)					
	ITOS	1-23-70	1,460 km (790 nmi) sun-synchronous (3 pm)					
Ranger	Ranger 3-5	-62	Translunar to impact	Lunar terrain	2.54-cm (1-in.) vid-ES	200	10	2.0
	Ranger 6-9	-65			2.54-cm (1-in.) vid-EM	700	2.56	200.0
Photo di-electric tape	Nimbus	Not flown	1,110 km (600 nmi) sun-synchronous (noon)	Visible cloud cover	35 mm D/C Tape	236.2/cm (600/inch) @ 50% response	3.25	650
OAO	Orbiting Astronomical Observatory	4-8-66	800 km (430 nmi) inclined	Telescope control	2.54-cm (1-in.) vidicon ES defl and foc	350	1.0	60.0
Apollo	Apollo 7, 8	-68	Translunar and lunar	Black and white real-time	2.54-cm (1-in.) hybrid vidicon	220	0.1	500.0
	Apollo 9, 11	-69		Black and white real-time	SEC hybrid	220	0.1	500.0
	Apollo 10, 11, 12, 13	-69		Color real-time	SEC-EM	360	0.033	4500[a]

[a] Limited to 1800 by communications link.

Table III.—(continued)

	Spacecraft	Dynamic range		SNR (peak signal rms noise), dB	Optics	Field of view		Exposure, ms	Weight		Power, W	Contractor	Reference
		lumen/m²-s [cd/m²]	ft-cd-s [f-L]			rad	deg		kg	lb			
TIROS	TIROX I-IX	0.22–10.76	0.02–1.0	40	5 mm f/1.5	1.832	105	1.5	4.717	10.4	11.6	RCA	2
AVCS	Nimbus	0.04–4.31	0.004–0.4	32	17 mm f/4	0.873	50	40.0	8.256	18.2	21.0	RCA	3
	TOS/ESSA			32	5.7 mm f/1.8	1.885	108	1.5	8.528	18.8	16.0		
	ITOS			32	5.7 mm f/1.8	1.885	108	1.5		18.8	16.0		
	Applications Technology Satellite (ATS)			40	200 mm f/4	0.052	3	40.0	10.297	22.7	31.0		
APT	TIROS	0.11–7.53	0.01–0.7	32	5.7 mm f/1.8	1.885	108	1.5	10.070	22.2	15.0	RCA	4
	Nimbus							40.0					
	TOS/ESSA							1.5					
	ITOS							1.5					
Ranger	Ranger 3-5	0.11–3.23	0.01–0.3	36	1016 mm f/5.6	0.009	0.5	20.0	2.722	6.0	5.2	RCA	5
	Ranger 6-9	0.04–7.32	0.004–0.68		76.0 mm f/2	0.209	12	5.0	7.893	17.4	30.7		
Photo dielectric tape	Nimbus	0.03–2.15	0.003–0.2	40	125 mm f/3.8	Panoramic		35.0	34.020	75	20 Write 25 Read	RCA	6
OAO	Orbiting Astronomical Observatory	7th – 2nd magnitude stars		43	76 mm f/0.87	0.209	12	No shutter	9.526	21.0	9.0	RCA	7
Apollo	Apollo 7, 8	0.03–322.92	0.003–30	43	8 mm f/2.0	1.396	80	No shutter	2.041	4.5	6.0	RCA	8
	Apollo 9, 11	0.003–13,557.60	0.0003–1260	40	25 mm f/4	0.611	35		3.289	7.25	6.5	Westinghouse	9
	Apollo 10, 11, 12, 13	0.323–4,304.00	0.03–400	43	25–150 mm (zoom)	0.122–0.733	7–42		5.897	13.0	16.0	Westinghouse	10

Table III.—(continued)

	Spacecraft	First launch date	Orbit	Application	Sensor	Horizontal resolution (TV lines)	Frame time, sec	Video bandwidth, kHz
RAE	Radio Astronomy Explorer (RAE)			Boom tip observation	1.27-cm (½-in.) vidicon EM defl and foc	—	13.11	2.5
RBV	Earth Resources Technology Satellite (ERTS)	(estimated) 1972	930 km (500 nmi) sun-synchronous (10 am)	Earth surface observation	5.08-cm (2-in.) RBV	4500	3.5	3000
Image Orthicon	ATS 4	-1968 (did not achieve orbit)	35,760 km (19,300 nmi) geostationary	Day-night cloud cover map	5.08-cm (2-in.) image orthicon	800	6.75	60
Image dissector	Nimbus	4-19-69	1,110 km (600 nmi) sun-synchronous (noon)	Visible cloud cover	2.54-cm (1-in.) image dissector S-11 surface	800	200	1.6
	ATS	11-5-67	35,760 km (19,300 nmi) geostationary			1300	13.3 min	28.0
NRL	Aerobee Rocket	11-4-69	Suborbital	X-UV solar flare observation	SEC tube EM defl and foc	450	0.033	4500
Surveyor	Surveyor	5-30-66	Lunar landing	Lunar terrain photography	2.54-cm (1-in.) hybrid vidicon	600 200	1.2 20.6	220 1.2
Mariner	Mariner 4	11-28-64	Mars flyby	Mars observation and survey	2.54-cm (1-in.) vidicon ES	200	24	6.94
	Mariner 6, 7	2-24-69			2.54-cm (1-in.) vidicon EM	945	42.24	9.45
Uvicon	Orbiting Astronomical Observatory	12-7-63	800 km (430 nmi) inclined	UV star maps	0.0000011-0.0000032 nm (1100-3200 A) Uvicons (4) Electrostatic	250	10.5	62
ATS	ATS 2, 4, 5	4-5-67	11,110 km (6,000 nmi) and 35,760 km (19,300 nmi)	Gravity gradient boom observation	2.54-cm (1-in.) vidicon	600	0.033	3500
DODGE	DODGE	7-1-67	35,760 km (19,300 nmi)	Attitude measurement; boom observation	2.54-cm (1-in.) vidicon	500	200	0.65
Redstone	MR-2	1-31-61	Boost phase	Booster stability and separation data	2.54-cm (1-in.) vidicon EM defl and foc	350	1/30	4.5
Saturn I	SA-5, 6, 7	1964	Boost phase	S-IV separation and ignition[b]	2.54-cm (1-in.) vidicon EM defl and foc	450	1/30	5.6
Saturn I	SA-8, 9	1965	~130 nmi	Pegasus deployment	2.54-cm (1-in.) vidicon EM defl and foc	450	1/30	5.6
Saturn IB	AS-202	8-25-66	Suborbit	Panel deployment	1.27-cm (½-in.) vidicon EM defl and foc	400	1/30	5.0
Saturn IB	AS-203	7-5-66	~120 nmi	Liquid hydrogen in orbit	2.54-cm (1-in.) vidicon EM defl and foc	550	1/30	7.0
FUTURE								
Skylab	Apollo Telescope Mount	Early 1973	235 nmi	Solar observation	Two 2.54-cm (1-in.) vidicons EM defl and foc	650	1/30	8.5
					Two SEC vidicons EM defl and foc	550	1/30	7.0

[b]Also, for SA-6, engine gimbaling.

Table III.—(continued)

	Spacecraft	Dynamic range		SNR (peak signal rms noise), dB	Optics	Field of view		Exposure, ms	Weight		Power, W	Contractor	Reference
		lumen/m²-s [cd/m²]	ft-cd-s [f-L]			rad	deg		kg	lb			
RAE	Radio Astronomy Explorer (RAE)	[685.2518–27,408 cd/m² (no shutter)]	[200–8000 fL (no shutter)]	—	5.5 mm f/1.8	1.047	60	No shutter	2.404	5.3	5.3	RCA	11
RBV	Earth Resources Technology Satellite (ERTS)	0.038–3.766	0.0035–0.35	35	126 mm f/2.8	0.279	16	12	21.773	48	50	RCA	12
Image Orthicon	(ATS)4	[0.0003426–34260.00 cd/m²]	[10^{-4}–10^{4} fL]	80	16.25 mm f/6.4	0.074	4.25	30–6630.0	30.845	68.0	50.0	Hazeltine	12
Image dissector	Nimbus	[68.520–34,260.00 cd/m²]	[20–10,000 fL]	40	5.7 mm f/3	1.571	90	No shutter	5.670	12.5	12.0	ITT	13
	ATS	[1,713.00–34,260.00 cd/m²]	[500–10,000 fL]		49 mm f/2	0.255	14.6		9.072	20.0	20.0		
NRL	Aerobee Rocket		—	38	80 cm f/9.3	0.031	1.8	30–2000	3.629	8.0	8.0	Westinghouse	14
Surveyor	Surveyor	[0.027–8,907.60 cd/m²]	[0.008–2600 fL]	36	25–100 mm f/4 (zoom)	0.105–0.436	6–25	150	8.301	18.3	10.2 (without heater)	Hughes	15
Mariner	Mariner 4	0.054–6.456	0.005–0.6	40	30.5 cm f/8	0.018	1.05	200	5.126	11.3	8.0	JPL	16
	Mariner 6, 7	0.022–4.304	0.002–0.4	45	50 mm f/5.6 500 mm f/2.35	0.192 and 0.019	11 and 1.1	90–180 6–12	21.727	47.9	29.0	EOS	17
Uvicon	Orbiting Astronomical Observatory	107,600.00:1	10^{4}:1	16	610 mm f/2	0.035	2	No shutter			25.0	EMR	18
ATS	ATS 2, 4, 5			35	10 mm f/	1.396	80	No shutter	3.175	7	10	Lear Siegler	19
DODGE	DODGE	[685.200–34,260.00 cd/m²]	[200–10^{4} fL]	25	6.5 mm f/2.5 18 mm f/2.5	1.396 0.524	80 30	1,000	8.618	19.0	9.	APL	20
Redstone	MR-2	10.7–10.7 × 10^{4}	1.0 to 10^{4}	32	6.2 mm f/1.5		30 × 45	33	2.73	6.0	18	Lockheed	
Saturn I	SA-5, 6, 7	5.4–10.7 × 10^{4}	0.5 to 10^{4}	32	12.5 mm f/2.5		17 × 23.5	33	5.0	11.0	14	Lear Siegler	
Saturn I	SA-8, 9	5.4–10.7 × 10^{4}	0.5 to 10^{4}	32	5.7 mm f/1.8		80 × 96	33	5.0	11.0	14	Lear Siegler	
Saturn IB	AS-202	5.4–10.7 × 10^{4}	0.5 to 10^{4}	28	8.0 mm f/1.8		47 × 60	33	4.09	9.0	15	GEC[c]	
Saturn IB	AS-203	5.4–10.7 × 10^{4}	0.5 to 10^{4}	40	12.5 mm f/2.5		17 × 23.5	33	4.09	9.0	15	MSFC	
FUTURE													
Skylab	Apollo Telescope Mount	Two vidicons Two SEC vidicons		43 36	Telescope Telescope			33 33	19.2 22.7		18 18	MSFC MSFC	

[c]General Electrodynamics Corporation.

Table IV.—Mechanical Scanner

Type	Spacecraft	First launch date	Orbit	Application	Scan	
					Type and scan angle	Instantaneous FOV, (mr) (spectral band designation)
High-Resolution Infrared Radiometer (HRIR)	Nimbus I, II, III	8-28-64	1110 km (600 nmi) polar sun-synchronous (noon)	Day–night cloud maps and cloud temperature	Cross-course rotating mirror (45 r/min), 2.059 rad (118 deg)	7.5
Medium-Resolution IR Radiometer (MRIR)	Nimbus II, III	5-15-66 (II)	1110 km (600 nmi) polar sun-synchronous (noon)	Albedo, water vapor and CO_2 distribution, day and night cloud maps, and cloud temperature.	Cross-course rotating mirror (8 r/min), 2.059 rad (118 deg)	43(A-E)[a]
Spin-Scan Cloud Camera (SSCC)	ATS I	12-6-66	Geostationary	Daytime cloud cover maps	Spacecraft spin (100 r/min) and latitude step of telescope, 0.314 rad (18 deg)	0.1
Multi-color Spin-Scan Cloud Camera (MSSCC)	ATS III	11-5-67	Geostationary	Three-color daytime cloud cover maps	Spacecraft spin (100 r/min) and latitude step of mirror 0.314 rad (18 deg)	0.1(A-C)
High-Resolution Scanning Radiometer (HRSR)	ITOS	1-23-70	1460 km (790 nmi) polar sun-synchronous (3 p.m.)	Day–night cloud maps and cloud temperature	Cross-course rotating mirror (48 r/min), 1.920 rad (110 deg)	2.7(A) 5.6(B)
Temperature-Humidity IR Radiometer (THIR)	Nimbus IV	4-8-70	1110 km (600 nmi) polar sun-synchronous (noon)	Water vapor distribution, day–night cloud maps, and cloud temperature	Cross-course rotating mirror (48 r/min), 2.059 rad (118 deg)	7(B) 21(A)
Multispectral Scanner (MSS)	ERTS A, B	First quarter, 1972	930 km (500 nmi) polar sun-synchronous (10 a.m.)	Earth resources survey	Cross-course oscillating mirror (15 Hz), 0.202 rad (11.6 deg)	0.077(A-D) 0.2(E)
Imaging Photopolarimeter	Pioneer F, G	First quarter, 1972	Jupiter flyby at 203,830.00 km (110,000 nmi)	Photometry and polarization of zodiacal light, asteroids, and Jupiter. Two-color mapping of Jupiter	Spacecraft spin (4.8 r/min) and cone angle step of telescope, 0.506 rad (29 deg)	0.5(A, B)
Visible-IR Spin-Scan Radiometer (VISSR)	Synchronous Meteorological Satellite (SMS)	Second quarter, 1972	Geostationary	High-resolution day and night cloud maps and temperature	Spacecraft spin (100 r/min) and latitude step of mirror, 0.314 rad (18 deg)	0.025(A) 0.2(B)
Very-High-Resolution Radiometer (VHRR)	ITOS-D	First quarter, 1972	1,460 km (790 nmi) polar sun-synchronous (3 p.m.)	High-resolution day and night cloud maps, and temperature	Cross-scan rotating mirror (400 r/min), 2.007 rad (115 deg)	0.6
Facsimile	Ranger			Lunar surface photo	Nodding mirror, camera rotation	1.5
	Explorer			Antenna position monitor	Rotating, nodding mirror 6.282 rad (360 deg)	2.3
Surface Composition Mapping Radiometer (SCMR)	NIMBUS E	First quarter, 1972	1,110 km (600 nmi) polar sun-synchronous (noon)	High-resolution maps of terrestrial mineral characteristics	Cross-scan rotating mirror (600 r/min), 1.571 rad (90 deg)	0.6
Very-High Resolution Radiometer (VHRR)	ATS-F	Fourth quarter, 1972	Geostationary	High-resolution day and night cloud maps	Raster scan of servo-stepped, gimballed flat mirror	0.3(A) 0.15(B)

[a] Letters in parentheses refer to respective channels of multispectral scanners.

Table IV.—(continued)

Type	Spacecraft	Optics aperture and focal ratio (including relay and immersion optics)	Detector type (spectral band)	Information bandwidth	System dynamic range blackbody temperature K; Earth albedo, %; Effective bright scene radiance range
High-Resolution Infrared Radiometer (HRIR)	Nimbus I, II, III	10.16 cm (4 in.): f/0.95 Cassegrain	PbSe photoconductor	300 Hz	200-340 K (night) 35×10^{-3} W cm^{-2} sr^{-1} (day)
Medium-Resolution IR Radiometer (MRIR)	Nimbus II, III	4.37 cm (1.72 in.): f/0.27 (B, D, E) 4.37 cm (1.72 in.): f/0.9 (A, C) Cassegrain	Thermistor bolometer	4 Hz (A-E)	0–80% (A) 0-270 K (B), 0-330 K (C) 0-270 K (D), 0-290 K (E)
Spin-Scan Cloud Camera (SSCC)	ATS I	12.70 cm (5 in.): f/2 folded paraboloid	S-11 PMT	160 kHz	≥1000:1
Multi-color Spin-Scan Cloud Camera (MSSCC)	ATS III	12.70 cm (5 in.): f/3 Wynne-Rosin	S-11 PMT (A, B) S-20 PMT (C)	160 kHz (A, B, C)	≥1000:1 (A, B, C)
High-Resolution Scanning Radiometer (HRSR)	ITOS	12.70 cm (5 in.): f/3.4 (A) 12.70 cm (5 in.): f/0.25 (B) Cassegrain	Silicon photodiode (A) Thermistor bolometer (B)	910 Hz (A) 455 Hz (B)	0–80% (A) 0-330 K (B)
Temperature-Humidity IR Radiometer (THIR)	Nimbus IV	12.70 cm (5 in.): f/0.24 (A), 12.70 cm (5 in.): f/0.26 (B) Cassegrain	Thermistor bolometer (A, B)	115 Hz (A) 345 Hz (B)	0-270 K (A) 0-330 K (B)
Multispectral Scanner (MSS)	ERTS A, B	22.86 cm (9 in.): f/3.6 (A-D) 22.86 cm (9 in.): f/2 (E) Ritchey-Chretien	S-20 PMT (A, B) S-25 PMT (C) Si PD (D) HgCdTe (E)	35.5 kHz (A-D) 13.7 kHz (E)	27×10^{-4} (A), 22×10^{-4} (B) 17×10^{-4} (C), 28×10^{-4} (D) W cm^{-2} sr^{-1} 0-310 K (E)
Imaging Photopolarimeter	Pioneer F, G	2.54 cm (1 in.): f/3 Maksutov	S-20 Channel multiplier (A, B)	500 Hz (A, B)	8×10^{-5} (A), 4×10^{-5} (B) W cm^{-2} sr^{-1}
Visible-IR Spin-Scan Radiometer (VISSR)	Synchronous Meteorological Satellite (SMS)	40.64 cm (16 in.): f/6.3 (A) 40.64 cm (16 in.): f/1.3 (B) Ritchey-Chretien	S-20 PMT (A) HgCdTe photoconductor (B)	210 kHz (A) 26 kHz (B)	0–80% (A) 0-320 K (B)
Very-High-Resolution Radiometer (VHRR)	ITOS-D	12.70 cm (5 in.): f/0.89 Dall-Kirkham	Silicon photodiode (A) HgCdTe photoconductor (B)	35 kHz	0.5–80% (A) 180-315 K (B)
Facsimile	Ranger	0.36 cm (0.14 in.): f/2.4	Silicon	100 Hz	8.0–2500 μW cm^{-2} sr^{-1}
	Explorer	0.86 cm (0.34 in.): f/	Photodiode	2.5 kHz	8.5 to 2800 μW cm^{-2} sr^{-1}
Surface Composition Mapping Radiometer (SCMR)	NIMBUS E	20.32 cm (8 in.): f/0.92	HgCdTe (A, B)	50 kHz	257-330 K (A, B)
Very-High Resolution Radiometer (VHRR)	ATS-F	20.32 cm (8 in.): f/1.7	HgCdTe (A) Silicon photodiode (B)	1200 Hz	185-335 K (A) 1–100% (B)

Table IV.—(continued)

Type	Spacecraft	NE△T at scene temperature K or SNR at { scene albedo, %; irradiance, W cm^{-2} }	Scanner size		Total weight		Maximum power, W	Contractor	Reference
			cm	in.	kg	lb			
High-Resolution Infrared Radiometer (HRIR)	Nimbus I, II, III	0.22 K at 270 K (B) 0.23 K at 330 K (C) 0.20 K at 270 K (D) 0.26 K at 290 K (E)	25.40 × 40.64 × 22.86	10 × 16 × 9	8.62	19.0	4	ITT	21
Medium-Resolution IR Radiometer (MRIR)	Nimbus II, III		16.51 × 16.51 × 33.02	6.5 × 6.5 × 13	6.58	14.5	7.5	SBRC	22
Spin-Scan Cloud Camera (SSCC)	ATS I	>30 at 10^{-11} W cm^{-2}	25.40 × 27.94 × 43.18	10 × 11 × 17	9.07	20	21	SBRC	23
Multi-color Spin-Scan Cloud Camera (MSSCC)	ATS III	>30 at 10^{-11} W cm^{-2}	30.48 × 27.94 × 43.18	12 × 11 × 17	10.66	23.5	23	SBRC	24
High-Resolution Scanning Radiometer (HRSR)	ITOS	19 at 0.5% } (A) 3000 at 80% } 1.4 K at 185 K } (B) 0.3 K at 300 K }	16.26 × 40.39 × 21.34	6.4 × 15.9 × 8.4	8.30	18.3	6.5	SBRC	25
Temperature-Humidity IR Radiometer (THIR)	Nimbus IV	4 K at 185 K } (A) 0.2 K at 300 K } 1.5 K at 185 K } (B) 0.3 K at 300 K }	17.78 × 19.05 × 39.62	7 × 7.5 × 15.6	9.03	19.9	7.5	SBRC	26
Multispectral Scanner (MSS)	ERTS A, B	100 at 1.6 × 10^{-11} W cm^{-2} (A) 73 at 1.3 × 10^{-11} W cm^{-2} (B) 44 at 1.0 × 10^{-11} W cm^{-2} (C) 73 at 1.7 × 10^{-11} W cm^{-2} (D) 1.2 K at 310 K (E)	38.10 × 38.10 × 91.44	15 × 15 × 36	52.16	115	25	SBRC	27
Imaging Photopolarimeter	Pioneer F, G	25 at 2.2 × 10^{-11} W cm^{-2} (A) 25 at 1.1 × 10^{-11} W cm^{-2} (B)	17.78 × 38.10 × 15.24	7 × 15 × 6	4.08	9	4	SBRC	28
Visible-IR Spin-Scan Radiometer (VISSR)	Synchronous Meteorological Satellite (SMS)	3 at 0.5% (A) 1.7 K at 200 K } (B) 0.4 K at 300 K }	50.80 × 50.80 × 147.32	20 × 20 × 58	60.10	132.5	23	SBRC	29
Very-High-Resolution Radiometer (VHRR)	ITOS-D	20 at 0.5% (A) 1.5 K at 185 K } (B) 0.5 K at 300 K }	20.32 × 20.32 × 48.26	8 × 8 × 19	9.07	20	5.0	RCA	30
Facsimile	Ranger	3 at 5.6 × 10^{-11} W cm^{-2} (at limiting bandwidth	3.12 dia × 24.99	1.23 dia × 9.84	1.18	2.6	16	Philco-Ford	31
	Explorer	3 at 14.1 × 10^{-11} W cm^{-2} (at limiting bandwidth	3.81 dia × 16.51	1.5 dia × 6.5	0.50	1.1	3		32
Surface Composition Mapping Radiometer (SCMR)	NIMBUS E	1.0 K at 280 K	22.86 × 42.16 × 54.86	9 × 16.6 × 21.6	19.05	42	15	ITT	
Very-High Resolution Radiometer (VHRR)	ATS-F	1.0 K at 200 K (A) 30 at 1% (B)	67.31 × 53.34 × 38.10	26.5 × 21 × 15	27.22	60	35	ITT	

2.2.1 Standard Rate Cameras

Television cameras operating at standard broadcast rates have been used for spaceborne electronic imaging in only a few applications, where the real-time observation of motion was a paramount requirement. Thus, ruggedized 2.5-cm (1 in.) vidicon cameras were used to monitor rocket engine firings, to observe the sloshing and drift motions of liquid fuel in tanks through launch and zero gravity conditions, and to observe the dynamic and thermal bending of long booms, such as the gravity gradient booms on Applications Technology Satellites (ATS). Similarly, the demand for immediate public coverage of the Apollo manned flight to the moon led to several varieties of spaceborne cameras with broadcast compatibility. There an initial video bandwidth limitation of 0.5 MHz resulted in a monochrome vidicon camera operating at 10 frames per second into a ground-based scan-converter that converted the signal to broadcast rates. Later extension of the available video bandwidth allowed operation at 30 frames per second; the horizontal resolution was somewhat less than standard quality. When the rate of 30 frames per second was used for sequential color frames on Apollo 10, 11, and 12 (see section 2.2.5.), the presence of color partially compensated for the lack of resolution. Despite the reduced picture quality of this approach compared to slow-scan systems with scan converters, the broadcast compatibility for direct viewing of motion outweighs the loss of resolution.

2.2.2 Slow-Scan Television Cameras

With the limited primary electrical power constraining communications bandwidth in many spaceborne applications, system designs utilized the time-bandwidth product relationship to exchange increased frame time for decreased bandwidth at video baseband (and correspondingly decreased tape recorder and/or RF transmission bandwidth). A general expression for the noninterlaced single-frame systems is given by

$$T \cdot B = \frac{N_v N_h}{2K}$$

where

T = frame time in seconds

B = video bandwidth in hertz

N_v = active number of scan lines per frame

N_h = limiting horizontal resolution, lines

K = scan efficiency factor (<1) dependent upon line and frame synchronization method

Frame times ranging from fractions of seconds to hundreds of seconds presented two requirements not encountered in standard television: a storage surface which would retain the image for the

respective frame time, and a shutter to expose the surface for a time commensurate with the light level and image motion, the latter usually a function of the spacecraft linear and angular velocities. As indicated in table III, many of the cameras utilized vidicons that required a photoconductor with inherent storage and a mechanical shutter in the optical system; those cameras employing image section tubes such as the image orthicon could incorporate an electronic shutter. However, the storage property of the photoconductor also poses a limitation because of the residual image after readout, usually requiring special erase and prepare cycles before the next exposure (ref. 35).

Since these slow-scan television systems are usually applied in a snapshot rather than continuous mode, they are subject to the same reciprocal relationships of light level, exposure time, image motion, optics aperture, and image-surface sensitivity as photographic film cameras. The slow scan permits images of high resolution and tonal quality to be transmitted over narrow bandwidths at feasible power levels. Of course, the intermittent nature of the exposures precludes real-time observation and necessitates hard-copy recording or special scan-conversion receiving equipment for direct viewing. Image tubes employed to date in slow scan systems have included the vidicon, the secondary electron conduction (SEC) tube, the image orthicon, and the return-beam vidicon (RBV); see ref. 36. Each of these tubes has capabilities and limitations that make it preferable for particular applications.

The vidicon is the simplest device of these four, and because of its light weight, small size, and low power requirements it has been suitable for many applications. Vidicons require the least sophisticated circuitry and are less sensitive than the others to thermal variations and to power supply or circuit drift. They have been successfully ruggedized for launch and landing, and some have proved the ability to survive (not operating) the temperature extremes of lunar day and lunar night. The vidicon cameras of table III have incorporated all combinations of electromagnetic and electrostatic focus and deflection. In general, the electromagnetic types are used where resolution is a requisite and electrostatic types where weight and power limits are severe.

The SEC tube is suited for operation where a wide range of light levels is expected, including somewhat low levels (ref. 37). It approaches the sensitivity of the image orthicon and the circuit simplicity of the vidicon. A vidicon type of electron gun is employed either with a hybrid arrangement of electrostatic focus and magnetic deflection or with all-magnetic fields. Nearly complete discharge of the SEC target by the beam minimizes residual image and simplifies the operating cycle. While the tube can operate over a wide range of light levels, the original version can be catastrophically damaged by exposure to very bright light or a point of light in a dark field. Recent introduction of a mesh-supported target into the SEC tube has eliminated this type of totally destructive damage, but bright source objects may cause local burn spots.

The image orthicon is larger and, to provide stable performance, requires more complex circuitry than a vidicon. Its prime attribute is high sensitivity (see section 2.2.3.).

The return-beam vidicon (ref. 38) is used for special applications where very high resolution of several thousands of lines per frame is required (see section 2.2.4.).

2.2.3 Low-Light-Level Television Cameras

For mission applications where the scene brightness is below the approximately 0.343 cd/m^2 sensitivity limit of vidicon imaging tubes, several low-light-level television sensors have been developed to "see in the dark." Spurred in large measure by military requirements, progress in low-light-level television is steadily approaching the theoretical quantum limit where, even though every incoming photon excites an atom in the detector, there are too few photons to form an image within the available exposure time.

The first practical television camera tube developed specifically for low-light-level imaging was the image orthicon. Increased sensitivity was obtained both by electron multiplication in the image section of the tube and by an electron multiplier which amplifies the returned scanning beam. An image orthicon camera for day- and night-time cloud observations was designed for and launched on ATS-4, but failure to attain orbit precluded in-orbit evaluation of low-light-level performance. The salient characteristics of the camera are shown in table III. The 800-TV-line resolution at full daylight illumination drops to 400 TV lines at quarter moon.

In the mid-1960s the SEC target, which provided a total controllable gain of 100 to 300, was announced. Employing direct target plate readout as in a vidicon, rather than electron multiplication of the return beam as in the image orthicon, the SEC tube demonstrates reduced sensitivity but higher resolution than an image orthicon of the same tube size. However, its relative simplicity of circuitry and stability of operation make it preferable to the image orthicon for space applications. Both the black-and-white and color cameras of Apollos 9, 10, 11, 12 and 13 have used SEC tubes, as shown in table III. One additional technique has been used to provide low-light-level capability in a spaceborne electronic imaging system, namely extended light integration capability as employed in the Surveyor camera. When the shutter was opened for exposures of 1.2 s to 30 min, lunar surface images were obtained in the dark phase of the moon at scene luminances down to 0.027 cd/m^2 of reflected light from the earth (ref. 39).

The extremely high sensitivity of low-light-level television cameras frequently requires use of sophisticated techniques to cope with the wide range of input light levels that may be encountered. Circuitry is required to sense average or peak illumination to control the gain of the tube or aperture of the optics. For example, the ATS-4 image orthicon camera contained a continuously variable neutral density filter arrangement which provided control of sensor illumination over a 10^6:1 range, while the SEC cameras controlled the high-voltage accelerating potential to adjust target gain. Another example of automatic gain control occurred in the Mariner 6 and 7 spacecraft (ref. 17). Each spacecraft had two cameras, one wide-angle and one narrow-angle, which took pictures successively. The wide-angle pictures overlapped, and the narrow-angle picture was located in the overlap area. The video data from the overlap area of one wide-angle picture automatically controlled exposure time on the following pair of narrow-angle and wide-angle pictures.

Intensifier sections have been evaluated for application to various types of image tube sensors, but none has been used in spaceborne imaging systems to date. Although an intensifier section in conjunction with one of the low-light-level cameras described could nearly achieve the quantum limit, the further loss of resolution has outweighed the advantage of ultrasensitivity.

A new low-light-level sensor, the silicon intensifier target sensor (SIT), has been developed recently and will be used in color cameras currently being fabricated for some of the later Apollo missions. The SIT combines a silicon diode vidicon with an image section whose signal is generated by optical inputs to a photocathode. The electron image, accelerated toward the silicon target, bombards it, and in so doing releases sufficient carriers to produce a charge gain in excess of 2500; very high sensitivity is the result. Limiting horizontal resolution of 600 TV lines is achieved with the 2.54-cm (diameter) vidicon and intensifier. Other features are inherent ruggedness, freedom from microphonics, and ability to absorb severe overloads in light input without damage. The image section may be controlled to provide a wide range of automatic light control. A variation of this approach of coupling an intensifier with a vidicon, incorporating electronic shuttering and electronic image-motion compensation in the image section, is being developed for the Viking 1975 spacecraft.

2.2.4 High-Resolution Television Cameras

Of the several approaches to achieving very-high-resolution images electronically, two fall within the Type I category of table I (the high-resolution image dissector is included under Type II, section 2.3.1, and mechanical scanners of Types IV and V are included in section 2.4). Much of the same technology has been applied to the development of the dielectric tape camera and the return-beam vidicon, particularly those aspects concerning the electron optics for magnetic focus and deflection of the high-resolution beam and the long retention photoconductor; in effect, the dielectric tape camera rolls up the photoconductor on a strip of Mylar tape to permit successive exposures before readout with the charge pattern corresponding to the image being stored in an insulating layer adjacent to the photoconductor. Development of a panoramic scan version was funded by NASA through prototype qualification, but the tape camera has not been committed to flight.

Resolutions greater than 100 line pairs per millimeter (lp/mm) on the photoconductor have been achieved in controlled laboratory conditions, but practical performance levels approach 90 lp/mm for vidicon readout and 80 lp/mm for an entire system (see section 3.2 and Appendix A). With a return-beam vidicon of the size contained in a 5.08-cm-diam envelope, a square scanning raster of 25 mm per side is used to provide 2000 lp or 4000 TV lines per frame. Systems incorporating 11.43-cm tubes with limiting resolution of 8000 lines are under development.

The high-resolution return-beam vidicon has the advantage over the image dissector and mechanical scanners of being a storage device capable of integration of luminous energy, hence ultimately greater sensitivity. Unlike the noise limitation of the standard vidicon, whose signal-to-noise ratio is determined by the necessarily high input resistance and pickup of the pre-amplifier for the target output signal, the return-beam vidicon noise limitation is that of the electron beam itself: initial amplification of the return-beam signal from the photoconductor by an integral electron multiplier provides approximately an order of magnitude of improvement in signal-to-noise ratio for the wide video bandwidth associated with high-resolution applications.

In applications of very-high-resolution image tubes, it is necessary that the beam be controlled to land accurately at a given spot, which moves over the raster as a function of time, with a given

velocity and direction. The accuracy of hitting the desired spot will determine the geometric accuracy. It is generally desirable that a maximum deviation of ½ scan line relative displacement be maintained on a short-time line-to-line basis, requiring that fluctuations in sweep generator and deflection amplifier gain be 80 to 85 dB below the sweep signal. Longer-term fluctuations and power supply effects can be maintained to control accuracy of size and centering to values of 1 to 2%. The velocity and direction of beam landing affect the shading, or local sensitivity, of the photoconductor. Correction circuits which both add to and multiply the video signal are employed to reduce this variation to less than 10%.

As with vidicons in general, the performance of the high-resolution return-beam vidicon, with respect to sensitivity, resolution, shading, and storage, is affected by the temperature environment. While the magnitude of these effects on the vidicon is less than that for an image orthicon, it is necessary to control the faceplate temperature to preserve very high resolution; otherwise high temperatures ($>40°C$) cause increased dark current, reduced response, and resolution loss from lateral charge dispersion, while low temperatures ($<0°C$) cause a loss of signal level. Thermoelectric cooling can, however, maintain the faceplate to $22° \pm 5°C$.

The residual image limitation described in section 2.2.2 applies also to the high-resolution RBV. Typical applications demanding a minimum time between successive exposures, consistent with the bandwidth limitations on readout rate, require a fast-erase technique in which the faceplate is illuminated by flood lights. A "prepare" cycle is then executed to restore the charge on the photoconductor to a nominal value so that the beam sees the same potential as it would after many scans. Fast-erase may, however, introduce side effects of lower sensitivity and greater shading.

Another recently developed high-resolution sensor is the FPS (focus projection scan) vidicon (ref. 40) that is also capable of resolution in the order of thousands of television lines. It is not presently scheduled for any space mission.

2.2.5 Color Television Cameras

Color capability was added to the Surveyor system by means of a four-position color wheel (ref. 41). The color wheel design permitted one of several filter elements to be inserted into the optical path on command from the earth. One quadrant of the wheel was clear, while the other quadrants contained three primary filters selected to shape the overall spectral response of the camera and filters. To maintain colorimetric calibration and enhance the detection of color differences, photometric targets were mounted on the spacecraft. These targets had three colors of purity and dominant wavelength that corresponded to the range of anticipated lunar rock colors.

The only use of real-time color television techniques has been in the Apollo program, where the camera was designed to provide real-time data from the command module and from the lunar surface. In order to keep the space hardware relatively simple, a single-tube television camera was synchronized with a rotating color wheel to generate a field sequential color signal. Translation of this signal to the National Television System Committee (NTSC) compatible broadcast format was performed on the ground by a scan converter.

The camera color wheel had six sections comprising two sets of red, green, and blue filters which were interference depositions selected for maximum transmission and desired spectral response. Calibration of the color filter wheel with the S-20 photocathode of the SEC tube provided fidelity for spectral analysis of the scene by data reduction of the received video.

Transmission of the sequential color fields is at the standard broadcast rate of 59.94 fields per second. Thus, a full-color field for compatible NTSC transmission must be synthesized from three separate single-color fields by the ground-based scan converter, yielding an effective color field rate of 20 fields per second, which is then repeated three times to produce the 59.94 fields per second for broadcast.

The aforementioned susceptibility of the original type of SEC tube to destructive overloading by bright light was manifested during inadvertent pointing of the color television camera to the Sun by an astronaut while on the lunar surface. The use of mesh-supported SEC or silicon-target-tube types in future Apollo cameras should eliminate susceptibility to target burn completely.

2.3 Electronic Line Scanners

While the Type I spaceborne electronic imaging systems, like their earthbound antecedents, employed two-dimensional deflection of an electron beam over the image surface to generate an image, many space applications can utilize the linear or angular velocity of the spacecraft to generate one dimension of scan. The other direction of scan can then be achieved electronically, either by an image tube or a linear array of detectors, or mechanically (section 2.4). Restrictions on the use of this sensor type are generally imposed by spacecraft motion. Yaw or roll of the satellite during the several minutes that the scene is being scanned will cause geometric distortions. Also, on a spinning satellite, the effect of satellite nutation is a displacement in the track of a radial element such that adjacent lines of information might diverge or overlap somewhat.

2.3.1 Image Tubes

The image tube that has found application for line scan cameras is the image dissector, a type of photomultiplier in which the sensitive area may be sampled by electronic scanning means (ref. 40). Excitation of the photocathode by light causes electrons to be emitted in direct proportion to the light level (in contrast to the vidicon mechanism of variation of the conductivity of the photoconductor). The size of the aperture which samples the deflected electron image is the resolution limiting factor, with values of 35 television lines per millimeter being achieved in practice with a 0.025-mm aperture.

Image dissector line-scan cameras have been used where motion of the vehicle supplied the second component of scan, orbital motion in the case of low-altitude spacecraft and vehicle spin in the case of synchronous spacecraft (ref. 42). The capability of the image dissector in a slow scan application is enhanced as the scan rate is decreased, giving increasingly more exposure in the sampled part of the image. Since the signal-to-noise ratio increases as the square root of the

sampling time, image quality is improved. Because the noise current is proportional to the square root of the signal, a complimentary capability of the tube is the near lack of background sensor noise, permitting operation at very low signal levels and allowing a wide dynamic range of operation. Electronic gain control can be utilized with the wide dynamic range of operation to normalize highlight video over 20:1 changes in scene lighting. The image dissector line scan camera features simplicity of construction, since there is no thermionic cathode, mechanical shutter, or iris, as on most of the frame cameras.

The lack of light integration by the photo surface in the image dissector places an upper limit on the scan rates such that a crossover exists between a frame tube with integration and the image dissector. The signal-to-noise ratio of the dissector is inversely proportional to the square root of the scan rate, while for a vidicon it is nearly proportional to the square root of the scan rate (Appendix B).

2.3.2 Detector Arrays

The all-solid-state analog to the image dissector for line scan operations has received much interest, but the state of development is still limited. Silicon phototransistor mosaic arrays consisting of 200 by 256 elements have been fabricated along with high-density microelectronic digital readout circuitry. Currently 400 by 500 element mosaics (with readout circuitry) are being made for NASA with element center-to-center spacing of 0.1016 to 0.1270 mm. Response is directly proportional to the irradiance, peaking at 0.75 μm with 15% response at 1.0 μm. Signal-to-noise ratio is also directly proportional to the square root of the active area, wih typical values of 5:1 at a radiant power density input of 1.0 $\mu W/cm^2$ on an element of $10^{-6} cm^2$.

Linear arrays are also used to reduce the complexity, weight, and power of mechanical scanners by providing a number of scan lines during each scan cycle (see section 2.4.2).

2.4 Mechanical Scanners

The development of most mechanical scanners for spaceborne electronic imaging was motivated by, and accompanied, two corresponding advances in observational satellites.

First, introduction of an earth-oriented spacecraft platform in the Nimbus program, in contrast to prior spin-stabilized vehicles, opened the way for mechanical scanners which utilized the forward orbital motion of the spacecraft for scanning one dimension of a raster, and a rotating mirror for the other dimension at right angles to the orbital plane. The first spaceborne mechanical scanners operated at various infrared wavelengths beyond the limited spectral response of image tubes, but later designs included visible channels also.

Second, the development of a satellite (e.g., ATS-1) with its spin motion in an earth-synchronous orbit provided a situation where angular, rather than linear, motion of the spacecraft could generate the scan in one dimension. The first so-called spin-scan cameras to exploit this mode of

operation had visible spectral response only, but infrared versions are under current development. A somewhat different class of mechanical scanner camera, known as the facsimile camera has found use where there is neither linear nor angular motion between scene and camera. One version was built for Ranger spacecraft and was intended for a "hard" landing on the moon. Flight models of a second version are now being built for use on Explorer spacecraft. The facsimile camera uses two axes of mirror scanning to take, typically, a panoramic view of surrounding terrain. The camera for the Explorer spacecraft will provide visual monitoring of part of the spacecraft itself. Facsimile cameras are resistant to shock, being very small, light in weight, and using a solid-state (silicon) detector. They are also characterized by large dynamic range, insensitivity to damage from viewing the Sun, and freedom from optical distortion. Scan rates of a few minutes to 8 h have been realized for a single 360° picture. Sensitivity is lower than for systems using television tubes because of the ncessary use of nonintegrating detectors.

2.4.1 Infrared

Chronologically, the two Nimbus infrared radiometers (ref. 21) were the first mechanically scanned spaceborne electronic imaging systems. Both incorporated a continuously rotating plane mirror in front of the primary optics, as shown in figure 1. This arrangement is typical of the scanning principle employed in several of the systems listed in table IV. The mirror is mounted at an angle of 45° to its axis of rotation so that the scanning field of view of the detector (s) lies in a plane perpendicular to that axis. The fixed optical system and detector are then mounted colinear with, or parallel to, the rotational axis. This scanning method covers a wide field of view with constant angular resolution across the scan since the detector's elemental field of view is always on the optical axis.

However, because the useful scan is limited to the angle subtended by the earth, the bandwidth requirement in the video system is proportionally greater than that corresponding to the average information rate. Typically the "dead time" of the rotational period is used for other purposes.

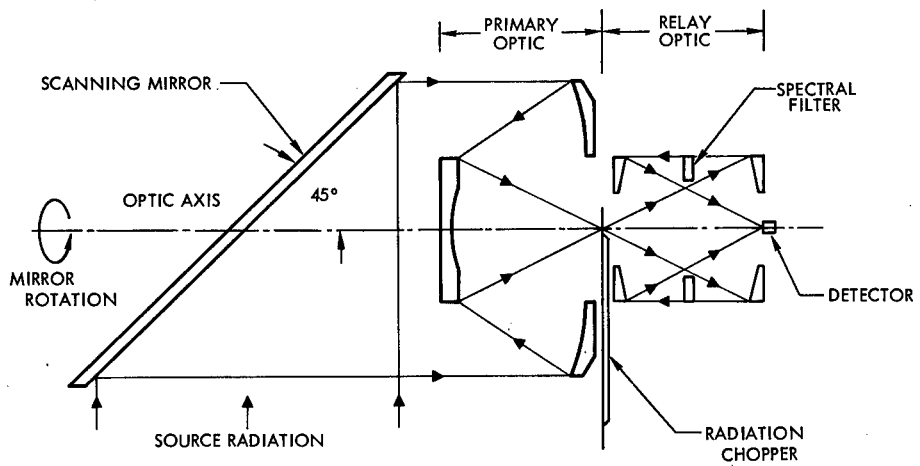

Figure 1.—Continuous rotation mechanical scanner.

It is usual to utilize the video signal derived from scanning the sky above the horizon as a cold calibration level for the thermal detector, and the signal from scanning the interior of the housing as a warm calibration level. Part of this inactive period is used for inserting telemetry and other calibrating information into the video signal.

The detectors located at the focal points of these scanners are subject to large output signal drift with small changes in ambient temperature and voltage bias; the incoming radiance is, therefore, interrupted periodically so that the ac component rather than the absolute value of the detector output is proportional to changes in the input irradiance. Most of the IR scanners have incorporated a mechanical "chopper" in the optical path, thus forming the video signal as amplitude modulation of the chopping frequency, which can be amplified by stable ac-coupled stages. A significant improvement in overall sensitivity and simplicity of the mechanism was achieved with the ITOS high-resolution scanning radiometer (HRSR) (ref. 25) in which the inherent alternation between earth and sky signals once per scan was used rather than high-frequency chopping. The standard television technique of video restoration was employed by clamping the known zero-radiance sky signal to a fixed reference on each scan. Drift is negligible over the approximately 1-s scan time, and the output signal during earth scan is then directly proportional to the absolute radiance level. Furthermore, the obtainable high-frequency response is improved since the detector time constant, instead of the chopping frequency, is the only limitation to the maximum video frequency. The chopping frequency, by sampling principles, must be at least twice the maximum video frequency, but in practice a factor of five (approximately) is used to provide adequate separation of the lower sideband from the baseband for demodulation.

The physical size of the mechanical scanning aperture, together with the requirement for infrared response, precluded sealing of the rotating mechanism in a pressurized enclosure with IR transmitting ports. All of the designs have therefore employed the technique of partial sealing by a noncontacting labyrinth around the shaft as shown in figure 2, with the scanning mirror, optics, and detector exposed. This labyrinth regulates the escape of lubricant, maintaining the internal pressure at the vapor pressure of the lubricant, which is stored in reservoirs of porous wicks or blocks. By itself or in conjunction with combinations of packed bearings, the vapor environment provides satisfactory lubrication of bearings and gears for lifetimes of several years. A problem common to this design is the contamination of the bearings from repeated pump down and backventing of the assembly during many ground vacuum test cycles. As the outside pressure is reduced, air in the gear/bearing enclosure vents out, but when the vacuum chamber is returned to atmospheric pressure any contaminants in the air flowing back through the labyrinth into the enclosure are likely to be trapped in the bearings. With the low torque levels and small clearances involved, even minute contamination can cause excessive drag and/or stall. Although bypass flow paths have been used with limited success, the only solution is to ensure that air vented into the chamber is clean and dry. Reduction gears with synchronous or stepping motor drive have been used on all scanners flown to date. Direct dc torque motor drives with tachometer or shaft position encoder feedback to maintain constant speed or constant step angle have been developed. A constant-speed drive is scheduled for the ITOS very high resolution radiometer (VHRR) and constant-step-angle drive is scheduled for the Synchronous Meteorological Satellite (SMS) visible IR spin-scan radiometer (VISSR) (table IV). Elimination of the gear train removes a source of wear, life limitation, and potential failure of the synchronous motor designs.

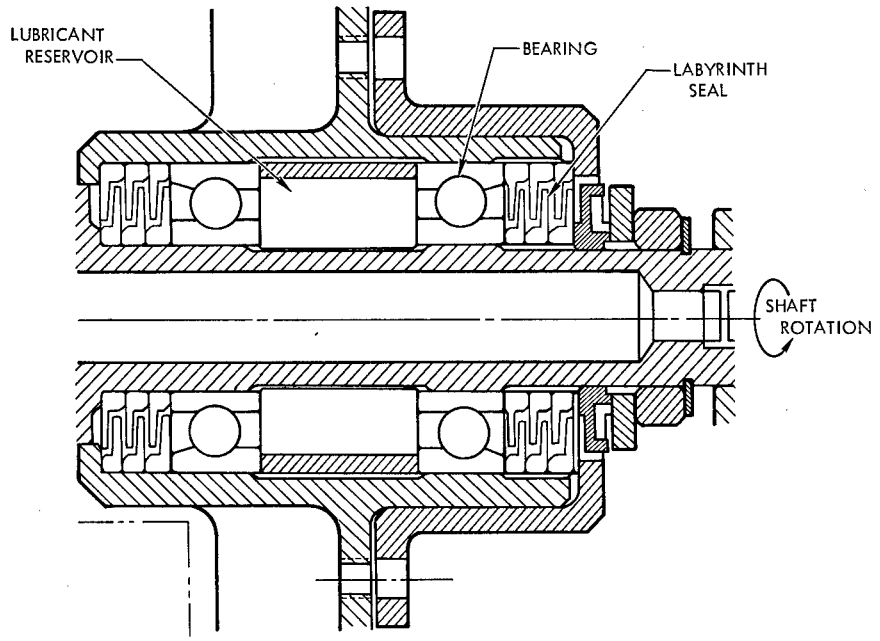

Figure 2.—Noncontacting labyrinth seal.

The original medium resolution IR radiometer (MRIR) was a multispectral imaging system, with all five channels extending into the infrared. Because of the overlap of some of the spectral bands, five separate telescopes were required, scanned by the single rotating mirror. Later systems such as the ITOS HRSR and VHRR employ two widely separated spectral bands in the visible and far infrared, allowing the use of a common optical collector with a dichroic beam-splitting filter to direct the respective portions of the incident energy on to the visible and infrared detectors. Because of the wide spectral coverage of these instruments, those optical elements common to all spectral bands must be reflective; not only does the spectral absorption of refractive elements limit their applicability, but correction of chromatic aberration over a wide spectral range is not practical, and the infrared self-emission from these elements can cause radiometric errors. The detectors used in the IR channels of these imaging systems operate at ambient or low temperatures, depending upon the sensitivity required (section 4.2), the low temperatures being achieved by passive radiation coolers.

An operational problem with wide-scanned field of view is the geometry of the orbit, which may result in sunlight striking some portion of the aperture even though not in the elemental field of view. Such sunlight impingement can warm the scanning or telescope mirrors and hence introduce a spurious signal to the thermal detector. The solution implemented on some designs is a sufficiently large sunshield to intercept the sunlight at these critical positions in the orbit. For the dual channel instruments, the sunshield and baffles must prevent energy from outside the field of view from reaching either the cooling patch or the detectors by any path with less than two internal reflections (from optically black finishes). Experience has also shown the necessity of employing materials for coatings, paints, finishes, and optics which undergo minimal, or known, change in characteristics under the prolonged exposure to solar and particle radiation in orbit; the sensitivity and performance of early TIROS radiometers degraded in orbit due

not only to change in surface properties but also to the condensation of outgassing products onto the optical surfaces (ref. 43). Similarly, a problem encountered on Nimbus 4 was the formation of water frost on a detector and cold patch; at the low vapor pressure at the cooler temperature of 195 K, absorbed water vaporized and recondensed on the cooler.

2.4.2 Visible

Three types of mechanical scanners have been developed specifically for visible electronic imaging: the spin-scan cloud cameras, the high-resolution multispectral scanners, and the facsimile cameras. The former were designed for daytime cloud cover mapping from synchronous altitude on the spinning Applications Technology Satellites, first as a single-channel monochrome camera, (ref. 23) and later in a three-channel color version (ref. 24). Spacecraft rotation at 100 rev/min provides constant-latitude scan lines (with 0.1-mr elemental field of view) with the scan position being indexed 0.13 mr each spin to provide the north-south coverage. Scan from approximately 50° N to 50° S in a 2000-line frame requires 20 min for the monochrome spin-scan camera, and pole-to-pole coverage in a 2400-line frame of the color spin-scan camera takes 24 min.

Two cross-flex pivots support the spin-scan camera telescope in the main housing and allow for the limited rotation to achieve latitudinal coverage. Flexural pivots do not require lubrication nor is there radial play which would introduce error in the step linearity and position repeatability. Latitudinal direction stepping of the telescope is accomplished by linear motion of a precision lead screw which is rotated 90° per step by a stepper motor and reduction gear. The entire drive assembly is lubricated, pressurized to 20 N/cm^2 (2 atm) with dry nitrogen, and sealed with rolling diaphragms at each end of the lead screw mechanism; the calculated leak rate of the diaphragms allows for at least 3 years of orbit operation.

Photomultipler tubes (PMT) are used for detectors in the spin scan cameras. The three photomultipliers used in the color version are mounted on the camera frame, rather than on the pivoting telescope as in the single-channel camera, to minimize the flexure load. Light is transferred from the focal plane field stop to the detectors by three flexible optical fibers of 0.0127-cm-diam each. Following the field stop, or fibers in the color camera, a diverging lens spreads the radiation onto the full diameter of the PMT, to reduce the flux density when the sun is scanned. Although both versions of the spin-scan camera employ a 12.70-cm-diam collector, the optical designs are different because of the color-correction and wide-field requirements of the three-color camera. Hard mounting of the optics is required to withstand the 6-g centrifugal load due to spacecraft rotation without any defocusing effects. Field stops in the focal plane are 0.0254 and 0.0381-mm pinholes in a thin metal sheet for the monochrome and color cameras, respectively.

The VISSR being developed for the Synchronous Meteorological Satellite is an extension of the spin-scan concept to combine long-wavelength infrared and visible imaging of high resolution. The telescope is mounted along the satellite spin axis with a servo-positioned 45° mirror being stepped 0.1 mrad per satellite spin to form the latitude scan in a 1750 line pole-to-pole frame. A linear array of eight fiber optics bundles at the prime focus relays the visible spectrum

energy to eight photomultiplers, realizing an elemental field of view of 0.025 mrad in the visible channel.

In addition, the prime focal plane is relayed by two germanium lenses to the infrared detector, with active command focus of these relay lenses required to adjust for the longitudinal shift of the infrared detector as the cooler stabilizes at its operating temperature of 80 K.

High-resolution multispectral scanners (MSS) under development for the Earth Resources Technology Satellite (ERTS) have four spectral bands in the visible and near-IR, although a long-wavelength channel is planned for addition on later models. A unique object-space scan mirror provides the 12° crosstrack scan at 15.2 scans per second. With a usable duty cycle of 65%, this oscillating motion for the narrow scan angle allows slower scan rate, and hence narrower electrical bandwidth and higher signal-to-noise ratios, for the given resolution than any of the constant-rotation mechanical scanners. This higher scan efficiency also provides correspondingly increased communications efficiency. Full angular momentum compensation of the mirror avoids attitude disturbances to the spacecraft. In addition to spectral separation into four visible and near-IR channels, a matrix of optical fiber ends clustered closely about the focal point of the telescope forms the field stops for scanning six lines at a time in each band illustrated in figure 3. Each fiber conducts the light from its instantaneous field of view to a corresponding detector, 18 PMTs being used in the three visible bands and six silicon photodiodes in the near-infrared. The high spatial resolution of the MSS necessitates tight mechanical and thermal tolerances of the Ritchey-Chretien optics assembly to maintain focus. Another special requirement is the mirror rigidity to maintain flatness under the large accelerations of reversal at the ends of each scan. In-orbit calibration is performed periodically by alternately deflecting sunlight into the focused area and shuttering to provide a dark reference.

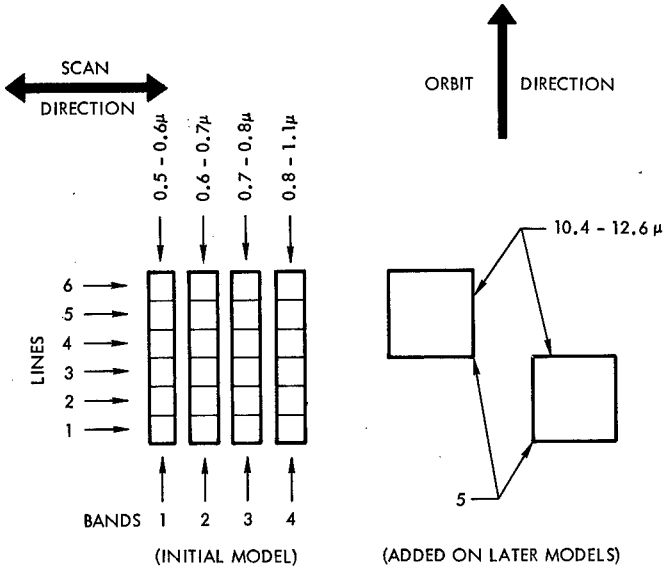

Figure 3.—ERTS multispectral scanner detector scan pattern.

3.0 Criteria

The criteria used in specifying and evaluating the design of a spaceborne electronic imaging system must treat the spaceborne hardware as a part of the total system which begins with the scene characteristics and ends with the hard or soft copy at the output. Thus, within the limits of physical realizability and economic reality, the desired quality and fidelity of the output with respect to the original scene shall be defined to derive the characteristics of the spaceborne electronic imaging system. In addition, the sources of spurious inputs to the total system, which may be before, in, or following the spaceborne imaging equipment, shall be identified and defined quantitatively so that the transfer function of the imaging system can be correctly determined.

3.1 Scene Characteristics

The scene parameters to be specified quantitatively shall include:

- Spectral distribution of incident illumination and reflectivity of various surfaces (ref. 44)
- Blackbody temperature and emissivity of various scene surfaces
- Attenuation and scattering properties of the transmission medium
- Spatial distribution of areas of different reflectivity or emissivity
- Range of energy levels (within a single scene, and from scene to scene)

3.2 System Transfer Characteristics

With the characteristics of the scene described analytically, the transfer characteristics of the spaceborne electronic imaging system shall be derived as a portion of the total system performance through the succeeding processes of recording, transmission, and display. Four major parameters that must be specified are:

- Energy transfer characteristic, incoming irradiance to electrical signal
- Modulation transfer characteristic (frequency response)
- Output signal-to-noise ratio
- Geometric fidelity of image

For the purpose of describing its performance analytically, the spaceborne electronic imaging system consists of:

- Optics, fixed (with shutter if present) or scanning
- Sensor, image tube or discrete detector(s)
- Amplifiers

Each of these three components has a modulation transfer function; both the sensor and the amplifying electronics have a noise figure; and the sensor has the important energy transfer characteristic.

3.2.1 Energy Transfer Characteristic

The energy transfer characteristic[1] of the sensor shall be specified as the output signal for a given exposure in a particular spectral interval. This relationship shall be verified by successive exposures to uniform scenes of varying radiance or luminance, with the results plotted on log–log coordinates to measure the nonlinearity. The slope of this curve is referred to as the gamma of the sensor.

3.2.2 Modulation Transfer Characteristic

The modulation transfer function (MTF) (Appendix B) of each of the three spaceborne imaging system components shall be specified as factors of the total system MTF; the MTF of the amplifying electronics shall include any effects of high-frequency peaking or aperture correction used to extend performance by offsetting some of the sensor high-frequency roll-off. In addition to cascading the three MTFs for a stationary scene, the motion of the imaging system with respect to the scene should be accounted for in its specification by introducing an equivalent MTF associated with image motion. Especially in considering the performance of high-resolution systems, the MTF of every component of the total system must be considered, not just the lowest. Since all electronic imaging systems entail some kind of raster scan to produce two-dimensional images, it is necessary to consider individually the MTFs parallel and normal to the line scan of the raster.

3.2.3 Signal-to-Noise Ratio

The noise of the imaging system shall be computed on the basis of an electrical bandwidth established by the specified angular resolution, the size of the total field of view, and the line scan rate (Appendix B). Sources to be considered are:

- Photon input (for very sensitive systems).
- Detector (electron beam noise, $1/f$ bias noise, and generation–recombination noise).
- Amplifier (usually determined by first stage).

[1]Also referred to as the amplitude transfer characteristic, the dc transfer characteristic, or the gamma curve.

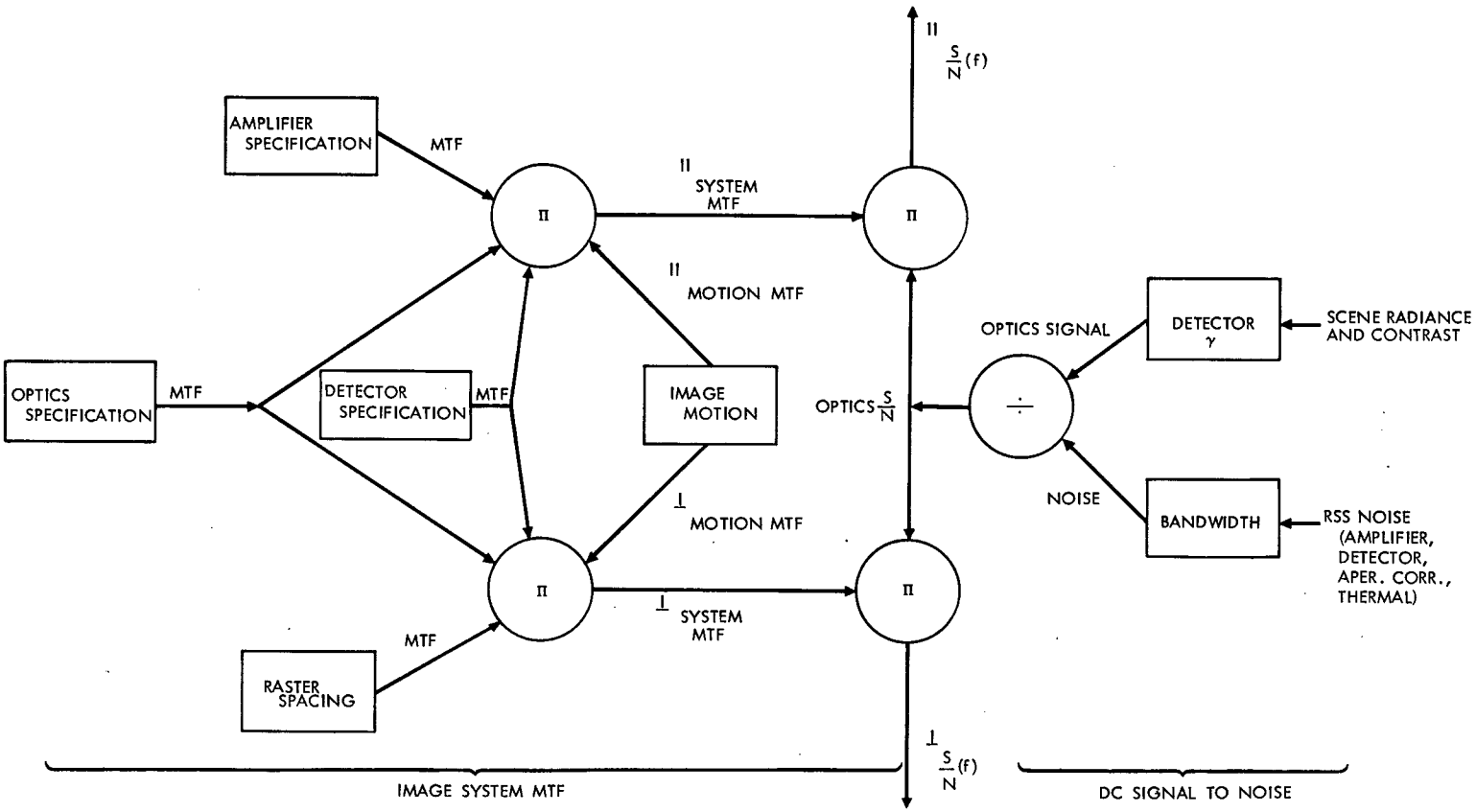

SYMBOLS II = PARALLEL AND ⊥ = NORMAL TO SCAN
f = CORRESPONDING SPATIAL AND TEMPORAL FREQUENCY
Π = PRODUCT

Figure 4.—Imaging system performance calculation.

3.2.4 Performance

Figure 4 summarizes the process of relating output signal quality to the scene characteristics by defining the MTF for each of the components of the imaging systems, the sensor gamma, and the noise sources. The output signal-to-noise ratio as a function of spatial frequency must be determined and used as a basis for target detection. To resolve a given spatial frequency, a spaceborne electronic imaging system shall produce a signal-to-noise ratio at its output proportionally greater than 4 dB by an amount (at that frequency) equal to the product of the MTFs of the succeeding system elements, namely, recording, transmission, and display (Appendix B). A noise source that should be considered with line scan imaging systems is aliasing (Appendix B).

3.3 Test Verification

Fulfillment of the design specifications of a spaceborne electronic imaging system shall be verified experimentally prior to flight. Simulated test scenes shall be used to obtain data over the appropriate ranges of:

- Irradiance (in the given spectral band) to obtain the energy transfer function
- Spatial frequency, to obtain the MTF

Signal-to-noise measurements shall be made at the output to confirm the resolving power.

Geometric fidelity shall be verified by imaging scenes of precise grids.

Careful consideration must be given to the verification of performance under environmental conditions similar to those expected in space, particularly measuring the change in performance over the required temperature range. The sequence of mechanical, thermal, and acoustic stresses and the degree of simultaneous exposure must be decided for each individual application.

4.0 Recommended Practices

The design of a spaceborne electronic imaging system should be treated as part of the design of a complete imaging system that includes recording, transmission, signal processing, and display components, and in which each effective aperture contributes to the composite system transfer function. After the necessary complete system transfer function is determined, a performance budget should be derived for: (1) the amplitude transfer function (gamma), (2) the modulation transfer function (frequency response), and (3) the signal-to-noise ratio, to obtain a reasonable balance of demands on designs of the several components. This process should insure that the spaceborne imaging component is neither an undue limitation on the total system nor an overdesigned device whose output quality cannot be preserved by the succeeding system components.

Reduction to hardware design of the respective amplitude and modulation transfer functions, within the particular spectral band and at the required signal-to-noise ratio, the practices outlined in the following sections should be considered.

4.1 Optical Design

The specification of the optical system for a spaceborne electronic imaging system must include the performance factors of MTF, spectral response and field of view as well as the primary physical factors of focal length, relative aperture, overall size and weight. Optical configurations may depend upon the spectral bandwidth of the imaging system with refractive (dioptric) optics suitable for visible applications and reflective (catoptric) optics suitable for very wide spectral bandwidth; i.e., far ultraviolet to far infrared; combined reflective and refractive (catadioptric) optics may be suitable for wide spectral bandwidth; i.e., near ultraviolet to near infrared applications.

The complexity of an optical system is in general determined by the required relative aperture or *f*/number of the system, the required field of view, the degree of color correction, and the MTF of the system. These same factors frequently determine the cost of the optical system, along with special parameters such as the use of aspherics, use of special glasses, or difficult-to-fabricate elements. As a rule, the lens having the highest angular resolution for a given spaceborne imaging system is the lowest *f*/number lens that can be carried such that its MTF, when combined with the MTF of the sensor and electronics, results in the highest possible imaging system MTF. In an aberration free system, the MTF and cutoff resolution are limited only by diffraction. This resolution limit (the Rayleigh diffraction limit) may be computed as:

$$\theta = 1.22\,\lambda/D, \text{ rad}$$

$$\Delta = (\lambda \times f/\text{number})^{-1} \text{ lp/mm at focal plane}$$

where

$$D = \text{aperture diameter, mm}$$

$$\lambda = \text{wavelength of focused energy, mm}$$

$$f/\text{number} = \text{effective focal length/diameter}$$

Decrease in the MTF due to changes in focus from relative displacements in the optical system from atmospheric pressure to vacuum as well as from variation in the refractive index of air to vacuum and thermal distortions and focus shift must be prevented by proper design and calibration.

The lens design may also be influenced by requirements of relative illumination. Most lenses exhibit a falloff in the illumination proportional to the fourth power of the cosine of the field of view. For wide angle lenses, such as the 110° types used on meteorological TV cameras, this falloff is large, and considerable complexity of extra optical elements is required to achieve a more uniform sensor illumination. Although a 50% dropoff at the corners of the image is quite acceptable for ordinary viewing, imaging systems utilized for metric analysis of the scene require a radiometric or light transfer calibration over the format, such as those performed on the Tiros, Surveyor and Mariner cameras.

The use of refractive optical elements for imaging requires color correction elements to maintain the MTF across the spectral band. Achromatic or two wavelength correction may be used, although apochromatic (three wavelength) or superachromatic (four wavelength) correction may be used where necessary. When several cameras are used for multispectral imaging, it may be necessary to have each lens designed for a particular wavelength to achieve maximum resolution

as in the ERTS RBV cameras. It is easier to correct for the red end of the spectrum than for the blue, because of the dispersion characteristics of glass.

Very wide band scanning systems for multispectral imaging may resort to catoptric optical systems which have no chromatic aberrations and whose transmission losses are a function of the spectral reflectivity of the mirror coatings. In these reflective systems, correction of geometrical aberrations must be done in the figuring of the mirror surfaces. Depending upon the degree of correction required over the field of view, the mirrors can range from relatively simple spherical and conic section surfaces; i.e., a parabola, to complex high-order aspherics with attendant problems in fabrication, mounting tolerance, thermal stability, and resistance to mechanical environmental stress. Although the reflective optics used in mechanical scanners have neither chromatic aberration nor, to any degree, off-axis illumination and MTF falloff, their requirement for surface geometrical figure accuracy introduces severe mechanical design requirements.

Mirror blanks may be made from special low coefficient of expansion materials such as CERVIT (made by Owens-Illinois), and ultra-low expansion (ULE) fused silica, and beryllium has been used in large mirror blanks because of its high stiffness-to-weight ratio. Much interest and effort have been given to developing bare beryllium polished finishes, but they appear to be no less a problem than the commonly used Kanigen electroless nickel coating and aluminized glass mirror surfaces. The Kanigen coating that is finally figured is difficult to produce as a uniform coating, and has a different thermal expansion coefficient from beryllium that can introduce sufficient stress to produce strain and loss of figure. Similarily, stresses from the mirror mount and the anistropy of beryllium must be carefully considered in the design to minimize loss of performance under environmental variations. Where a high surface figure is required, it is necessary that the mirror structure designs be based on the precision elastic limits rather than the yield strength used in structural applications (ref. 45).

Special attention must be paid to the spectral properties of coatings for both refractive and reflective optics, to light scattering from surface imperfections, and to the baffling of the complete optical system to reject extraneous radiation. To avoid loss of transmission from exposure to solar ultraviolet radiation and/or trapped particles in the Van Allen belts, fused silica and radiation-resistant glasses should be used for lenses, filter, and optical windows.

Mechanical shutters in the optics of image tube television cameras require adequate lubrication to operate for many thousands of cycles. Magnetically operated focal-plane shutters in Teflon guides have attained millions of cycles of operation, compared with only ten or twenty thousand cycles for iris shutters. Single-blade slit shutters are satisfactory for exposures of 1 to 5 ms while two-bladed shutters are required for longer exposures to obtain uniform exposure over the sensor surface. The microphonic effects of shutter operation on camera tube elements, particularly the vidicon mesh, must be evaluated in the shutter design.

Special precautions in design are also necessary to insure lubrication of zoom lenses and iris diaphragms when they are used; one particular precaution in the choice of mechanical design and lubricant is to avoid the recondensing of evaporated lubricant on any optical surfaces. In addition to the lubrication of moving optical components, follower potentiometers for the servo control must be lubricated to avoid cold-welding.

Aliasing can be reduced by shaping the pinhole aperture and by decreasing the azimuth stepping interval of the facsimile camera. When shaping the aperture (by lengthening its dimension along the azimuth direction), a careful tradeoff must be made with the reduced MTF. And when decreasing the angular azimuth stepping interval, a careful tradeoff must be made with the increased video data per image frame. Because of these important tradeoffs for spaceborne imaging systems, normal to line scan aliasing should be included as a performance criterion (see Appendix B).

4.2 Detector Selection

The critical component selection in a spaceborne electronic imaging system is usually the detector, which, in fact, often sets the limit of performance of the system. Since a tradeoff is inevitably necessary between the desired performance capability and other factors such as weight, power, reliability, and environmental compatibility, it is essential that the performance requirements of the total imaging system be clearly defined and that relative priorities be assigned to each. Once the system requirements have been established, as much information as possible should be acquired concerning the operation and features of each device so that a comparison can be made. Figure 5 shows the range of sensitivity and resolution for various image tubes and visible sensors (ref. 46), while figure 6 gives corresponding data for infrared detectors. Similar data should be obtained for the evaluation of new detectors as they are developed.

System designers must be supplied with the characteristics of each type of detector to be considered. In addition to the primary performance data of figures 5 and 6, the parameters listed below must be evaluated. Because the definitions, and hence the values, of some of these parameters vary throughout the industry, the definitions must be verified with the data.

Detector characteristics to be evaluated are:

(1) Responsivity and signal-to-noise ratio

(2) Resolution

(3) Dynamic range

(4) Spectral response

(5) Gamma

(6) Storage time/slow scan capability/residual signal

(7) Integration time/time constant

(8) Impedance

(9) Stability and uniformity

(10) Operating requirements

(11) Environmental susceptibility

(12) Physical characteristics

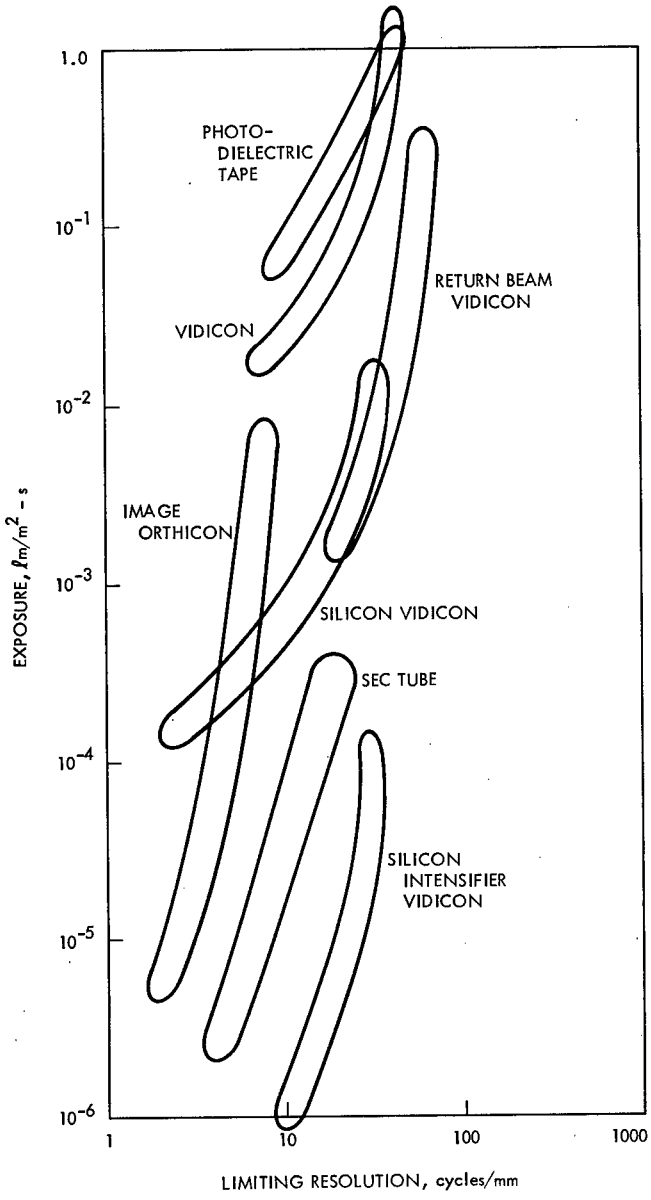

Figure 5.—Visible sensor sensitivity data.

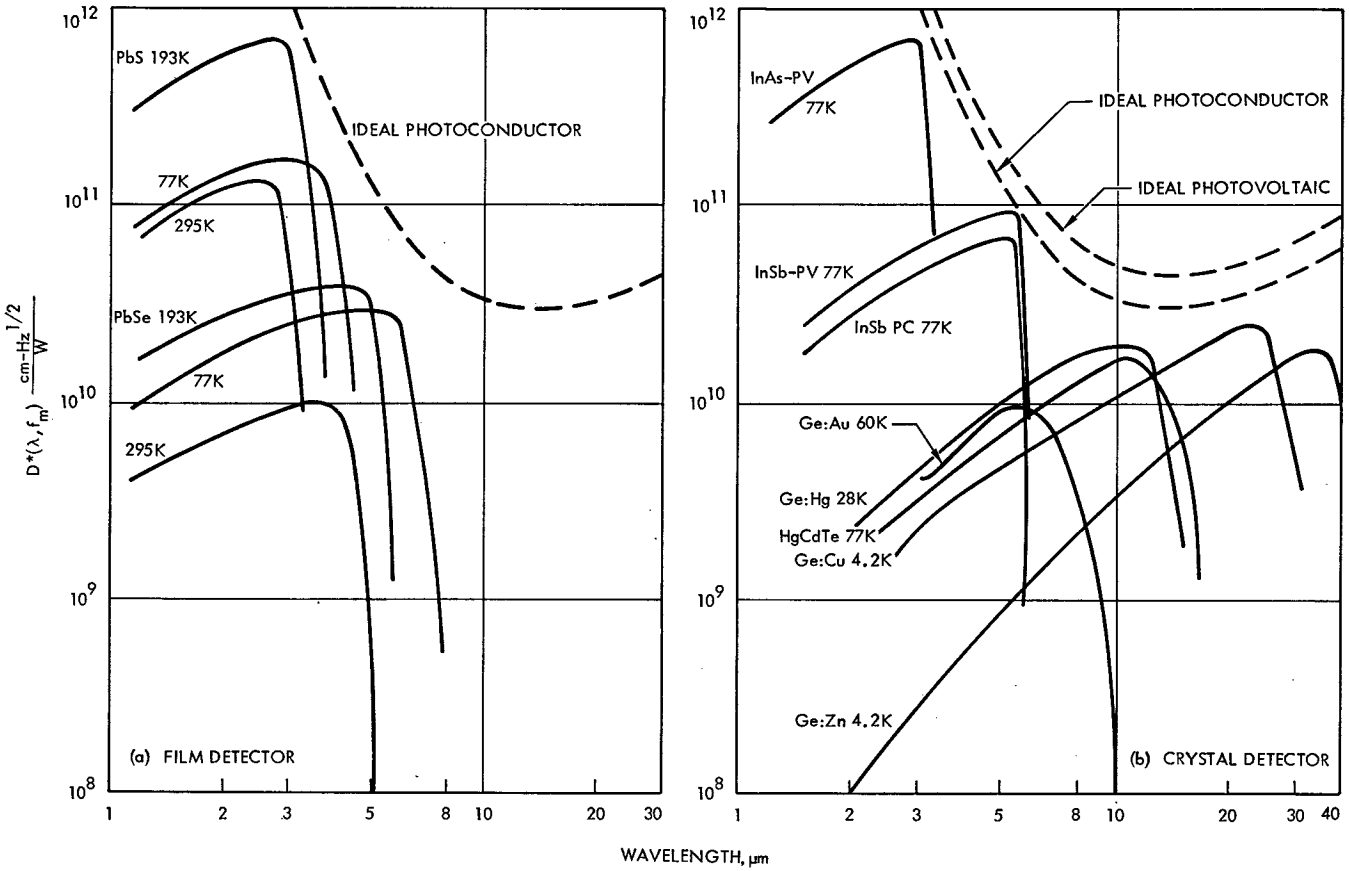

Figure 6.—Infrared detector responsivities; field of view = 2π sr, background temperature = 295 K.

Although responsivity of image tubes and photomultipliers is often given in microamperes per lumen or per watt, a more useful single-parameter characterization of the sensitivity for all types of detectors is the noise-equivalent irradiance, defined as the incident power density required to provide unity signal-to-noise ratio. For point-source imaging, e.g., of stars, the sensitivity data above are not generally applicable, and special measurements should be performed. Similarly, the manufacturer's responsivity data may not be valid for special applications involving non-standard techniques, such as beam chopping, target switching, extended erase, etc., used to improve performance. Rather than a single number for limiting resolution of the detector, the MTF should be combined with the MTFs of the other system elements to determine overall performance and resolving power.

For a given level and spectrum of irradiance, the signal output from a detector may vary with operating potentials or bias, temperature, time and location on the format for an image tube or array. The importance of these factors is related to the calibration method, particularly to the possibility of in-flight calibration. Some of the operating requirements may pose electronic design problems, such as high-voltage high-current stringent regulation of current or voltage (of the order of 0.01%) and linearity of sweep waveforms. For high-resolution image tubes, dynamic focus as a function of the position of deflection may be required. Detector stability is especially important in multispectral imaging systems, because relative response in the several channels must be preserved; image tubes and photomultiplier tubes must be operated at maximum current for as long as several hundred hours to stabilize their performance.

All detectors, whether image tubes, single crystals, or arrays, vary significantly in performance with temperature. In addition to operating variations, they must often survive very wide ranges of temperature, such as the exposure to lunar noon and night of the Surveyor camera, for which special cryogenic tests of the vidicons were employed to eliminate tubes whose photosensitive layers flaked off at low temperature. While most of the image tubes require an ambient operating temperature near 300°K, some of the IR film and crystal detectors have useful signal-to-noise ratios only at low temperatures, such as 200°K for the lead salts (sulfide and selenide) and 80 to 100°K for mercury cadmium telluride. The scanning image systems employing these detectors require coolers which for long-life missions, must be passive. Whatever the nominal operating temperature of the detector, temperature cycling between the upper and lower limits around the nominal is recommended to disclose potentially high-noise detectors.

The problems and limitations of solid-state detector arrays are more those of large-scale integrated circuits than of the detector technology per se. A fundamental problem is the accurate delineation of individual elements without physical or chemical damage to the detector material. Photoetching techniques have proved most satisfactory for both film and crystal arrays. With the integration of follower circuits on the same chip with the detector array, performance is limited by the noise figure of the high resistance of the follower bias circuit and the noise and physical characteristics of the wire bonds. At higher video frequencies, the stray capacitance between conductor traces may limit performance.

4.3 Electronic Design

New circuit designs for spaceborne electronic imaging systems must take into account the many variables and interacting factors introduced by a vacuum environment and radiation as well as by the functional performance requirements. Designs for circuits in space have too frequently revealed gross unfamiliarity with voltage breakdown and corona phenomena at low pressures (ref. 47) and lack of information on the chemical and physical behavior of materials in the space environment.

The principal environmental conditions that permit breakdown and corona in space are vacuum and radiation, which degrade electrical performance by: (1) degrading the insulating properties of materials, (2) outgassing dielectrics, and (3) providing a variable ambient pressure. To avoid the change in insulating properties by the loss of volatile components, modern insulating materials of the Teflon family should be used. The volatization of escaping gases from a solid, termed "outgassing," is observed for all organic insulators in vacuum, but the extent depends on the particular material and temperature involved. Outgassing presents a problem because it generates a slow-forming artificial atmosphere of unpredictable density that is difficult to evaluate in design equations. Teflon dielectrics and insulators have very low outgassing but tend to cold-flow under stress, while nylon has relatively high outgassing and should therefore be used with caution. Whatever the dielectrics used, the mechanical design of all electronics boxes that are not hermetically sealed should allow sufficient venting of the outgassing products to avoid buildup to critical pressure. Electrode spacing, size, and shape should be designed to minimize voltage gradients, which tend to induce corona and breakdown.

Good electronic design will reduce the possibility of corona discharge. If at all possible, an expert in high voltage and corona should work closely with circuit designers during the initial design phases and should also participate in the thermal vacuum testing. If an engineer who recognizes corona symptoms is not present, corona effects are often not noticed during such tests unless a catastrophic failure occurs. The following are specific recommended design practices.

Teflon-insulated cable should not be used for voltages greater than 250 V. Despite etching techniques, a reliable bond between the Teflon and the potting material (or conformal coating) is difficult to obtain. Potting (conformal coating) is generally used when a cable is terminated. When the potting material does not bond to the Teflon, an air gap is formed at the interface. In many cases the air gap takes a very long time to leak down to the critical pressure for corona. Thus, there exists a significant probability of not detecting such a potential corona source during thermal vacuum testing since such testing is usually accomplished over a much shorter time interval than the mission time period.

All high-voltage cables should be shielded to prevent possible corona discharges to neighboring low-voltage circuits, particularly those that employ semiconductors. The grounding of the shield should be arranged so that these discharge spikes do not propagate through the grounds of low-voltage circuitry. All high-voltage power supplies (if potted) should be shielded. The shield should be bonded to the outer surfaces of the potted power supply.

The use of shrinkable tubing in high-voltage circuitry should be avoided. The removal of air entrapped under this tubing is very difficult.

Test points should be provided for high-voltage monitoring during thermal vacuum testing as an aid to detecting incipient corona.

Exposure to the radiation of terrestrial belts and solar flux will cause changes in the characteristics of semiconductor circuit elements. Since 1960, considerable research has been performed to evaluate the surface and bulk damage effects in many types of semiconductors as a function of the dose rate and accumulated dosage of various kinds of radiation (refs. 48 and 49). After the expected dosage for a given mission is determined, the circuit design of the imaging system must employ an appropriate combination of: (1) selection of "hardened" (i.e., with minimum sensitivity to radiation) semiconductors from the available space-qualified parts lists, (2) allowance for indicated change in component characteristic, and (3) shielding by the metal of its own enclosure plus the surrounding spacecraft structure.

Functional design of the signal processing electronics of the imaging system must be treated as a contribution (and limitation) to the overall system modulation transfer function, distortion, and noise. Circuit design must provide for the variation in component values with temperature and time; operation at extreme temperatures may require active thermal control, such as the heaters embedded in circuit boards of the Surveyor camera. Not only must the high-frequency response contribution to the MTF be specified, but the low-frequency droop must be controlled to provide amplitude accuracy. This accuracy will also depend upon the stability of the reference voltages to which the video signal is clamped and upon the stability of amplifier gains which may be automatically switched to provide dynamic range. Also, the design and generation of the synchronizing signals require careful consideration to maintain the stability necessary to realize all the resolution of which the system is capable.

Generally added or mixed into the video waveform, the line sync signal should have its rise-time commensurate with the bandwidth of succeeding stages to prevent overshoot and "ringing." When used, amplitude sync pulses should be superimposed on constant-level intervals in the video signal, with a short delay or porch preceding each sync pulse; the porch ensures a constant sync rise-time to the sync detector in the ground equipment. Since many spaceborne imaging signals are transmitted both in forward (real-time) and reverse (recorded time) sequence, both front and back porches may be necessary for the sync pulses.

Particularly for the more sensitive detectors, noise due to front-end pickup can limit the system sensitivity, placing stringent requirements on the performance of the first preamplifier, which should, therefore, be as close to the detector as possible. Noise from the power supply converters of the imaging system should be minimized by suitable decoupling and grounding, and, where scan rates make it feasible, by synchronizing the converter switching with the blanking portion of the scan.

Successful design requires careful attention to the details of grounding and power distribution throughout the system. This problem should be approached by first considering the complete spacecraft and working back through the electronic imaging system down to the individual circuits. Lack of foresight in system grounding can result in months of "debugging" during system

integration and test, which, in turn, leads to trial-and-error solutions that are often marginal or constrained by other aspects of the design. Of the various methods of grounding, the single-point-ground and power-supply-feed method is the best means of preventing signal interference within complex systems. For this method to be successful, signal returns must not tie two physically separated ground points together, nor can chassis, shields, or structure be used for current-carrying circuit returns. Although it is not necessary to carry the single-point philosophy down to circuits on individual printed wiring boards or integrated circuit chips, the ground path should not carry current in a loop around the board. For amplifier stages, the ground should proceed, starting at the connector, from the highest-signal-level stage toward the lowest-level stage. Where a combination of a small capacitor and a large capacitor is used to achieve broadband decoupling, a resistor should be inserted between the two to eliminate the resonant effects between the capacitors and their lead inductances. When large converter spikes are present on a voltage line that is being filtered by an active regulator or Zener diode, reactive energy storage must be employed at the regulator input since the regulator cannot supply energy to remove the spikes.

Shielding may be necessary to contain radiation within an enclosure as well as to keep external energy from coupling into the protected circuits either electromagnetically, electrostatically, or magnetically. The type of shield design will be determined by the nature and frequency of the field. Careful attention to the construction of seams, joints, and mating surfaces is necessary for RF shielding, with a conductive gasket usually required around box covers for frequencies in the gigahertz range. Shields within wire bundles should be isolated from each other. Shielding from low-frequency magnetic fields due to spacecraft magnetic attitude control or spacecraft rotation within the earth's field is critical for magnetically focused or deflected image tubes; significant deflection and amplitude modulation of the first automatic picture taking (APT) camera pictures at spacecraft spin frequency led to the use of magnetic shields around the cameras on successive TIROS Operational System/Environmental Science Services Administration (TOS/ESSA) spacecraft.

4.4 Mechanical Design

The requirement for the mechanical design of a spaceborne electronic imaging system is to maintain the alignment and focus of the optics and detector over the full range of environmental conditions to which the system is exposed. Environmental conditions that the system must withstand include not only launch vibration and space vacuum, but the more severe qualification test levels of shock, acceleration, vibration, and temperature corresponding to the particular launch vehicle standards. Structural design for rigidity is straightforward although special techniques and materials must be employed to minimize weight. The vacuum and thermal stresses in the structure, however, present the greatest problem in mechanical design.

The mechanical design of the spaceborne imaging system must be closely coordinated with the total spacecraft design to define the mechanical tolerances and thermal interface necessary to preserve the alignment and focus of the imaging system. Particularly for large optical systems such as the scanners described in section 2.4, the structural stiffness of the telescope and spacecraft combination must be analyzed as a composite member to insure that no permanent deflections or strains that affect the alignment or focus are incurred during the launch and test

vibrations. Since test levels always exceed the expected launch loads to allow for a margin of safety, it is important that realistic levels, based on the expected environment, be used rather than arbitrarily high levels which penalize the design unnecessarily. To reduce mechanical environmental stress on the imaging system subassemblies, the transmissibility of the structure should be kept low. Necessary precautions relative to the vibration inputs to the optics-detector assembly also include the internal structure of image tube detectors, requiring ruggedized design and stiffening of elements to raise their resonant frequencies above 700 to 1000 Hz; hot cathode filaments are especially vulnerable. For those parts of the assembly where dimensional stability is not of paramount importance, bolted or riveted buildup will provide better structural damping than forged or machined one-piece construction.

The requirements for structural rigidity in the imaging system-spacecraft interface are usually conducive to close thermal coupling, tending to minimize temperature difference. However, because there is inevitably some heat flow through the imaging system and across the interface, with the direction perhaps changing with time as a function of orbit position and Sun/eclipse effects, finite thermal gradients will normally be present. Therefore, during the optics-sensor design, alignment can be preserved under thermal deflections both from temperature changes and gradients and from differences in material thermal coefficients by employing the same material in as much of the telescope frame and mount as possible, to avoid bimetallic effects. The thermal gradients can be reduced by maximizing the conductive and radiative coupling of the extremities of the mount. Resistance to both thermal and mechanical stress is enhanced by employing a high stiffness-to-weight material; beryllium has been successfully employed in some of the larger spaceborne electronic imaging system designs. The complexity of the thermal interface with the spacecraft has also led, in some designs, to thermal isolation of the imaging system from the spacecraft by multilayer blankets and insulators for radiative and conductive decoupling, respectively. Whether the spacecraft elements are tightly coupled or completely isolated, the design object is the same: to realize a configuration whose thermal behavior can be accurately characterized, thus maintaining thermal distortions within limits.

A second aspect of imaging system mechanical design is that encountered in several types of mechanisms that must operate in vacuum, often at very low gravitational levels. Solid lubrication of camera shutters by means of a plastic (such as Teflon) guide for the sliding shutter blade has been found satisfactory, although cold-flow properties may require special attention. For iris control and zoom motors and gears, which inherently are used very infrequently, silicone greases that maintain their lubricity over wide temperature ranges in vacuum usually serve adequately; for extreme temperatures, dry molybdenum disulfide or niobium diselenide lubricants may be preferable. However, mechanical scanner designs using bearings and/or gears for continuous operation require metal-to-metal lubrication. Even when a special treatment of the bearing surfaces, such as the application of Vac Kote,[2] is used, a partially sealed, enclosed design with reliable containment of lubricant is recommended; space-qualified seals and lubricants are available for such applications and should be used whenever possible. In the choice of drives, bearings, and lubricants, adequate torque margin must be provided to maintain uniformity of motion over the operating temperature range. A factor of five should be considered as minimum. All bearings should be tested for dynamic torque at operating speed, and bearing smoothness should be measured after prototype vibrations to verify the adequacy of the design.

[2]Ball Brothers Research Corp., Boulder, Colo.

When torsional suspension elements are employed as flexural pivots to avoid the lubrication problems of bearings and gears, they must be protected from launch stresses. Pivot fatigue, as well as change in the torsional spring constant over the operating temperature range, must be considered in the design. Lastly, only space-proved paints and finishes should be used. Any new coating or paint should be tested for its evaporation rate under space environment and for adhesion properties over the expected temperature range.

4.5 Alignment, Calibration, and Test

Since the images obtained from a spaceborne electronic imaging system are usually intended for various kinds of scientific and technical analysis, it is imperative that the performance of the final hardware be known, not only to verify the design but to provide a quantitative basis for the data analysis and picture enhancement. The measurement of system performance should include verification of each significant design parameter and interface characteristic, utilizing test stimuli and observables which, as closely as possible, simulate the total system application for the intended mission.

Alignment of the optical axis of the imaging system with respect to reference axes of the spacecraft, such as the spin axis or attitude-sensor coordinates, should be measured to about one-tenth of the specified alignment accuracy. This precision will provide corrections and refinements to be incorporated into the final data reduction and image analysis and will allow observation of any shifts in alignment as the system proceeds through its environmental tests—shifts that might indicate a trend toward misalignment, even though the actual shifts are small. Various autocollimating devices and auxiliary mirrors can be used for alignment of the optics and sensor of the imaging system, but it is preferable to perform the final alignment with the imaging system as nearly in its flight configuration as possible rather than to rely on a procedure that requires removal of a portion of the optics. Alignment targets are recommended that permit an image or a scan to be obtained through the system so that the alignment can be verified to the desired accuracy from the output image.

As scientific instruments, spaceborne electronic imaging systems may be used to obtain measurements of characteristics as disparate as size and distance, polarization, object texture and temperature, and material identification. Such characteristics are measured indirectly from the information that the imaging system can measure directly: namely, the projected areal distribution in the image plane of the amplitude of radiant energy of known polarization integrated over a known spectral range. Therefore, calibration requires ascertaining the system response to this information, utilizing known input stimuli while the variable parameters of the imaging system are known and fixed. The calibration should be performed with the entire system in operation and without nonflight interface equipment. The characteristics calibrated may be grouped under photometry or radiometry, geometry, and resolution. Radiometric calibration is the determination of amplitude response over the image format to the total range of irradiance from the anticipated scenes; this response must be known for the variable gain or sensitivity conditions of the imaging system including selection of filters, aperture, and exposure time. Calibration sources of known spectral distribution, polarization, and magnitude are required to provide an absolute radiometric accuracy of 5%, considered necessary for the majority of space imaging

applications; in a few specialized applications, such as albedo measurement for heat balance computations and temperature measurement for profile determination, accuracies of 1% are necessary. Geometric calibration entails measurement of the linearity of scene-to-image conformal mapping over the image format. Resolution calibration is the measure of the system's ability to resolve detail; it should be performed by measuring the MTF of the imaging system, thus providing corrections that can be used in the later processing of the returned data.

The MTF of the imaging system is obtained by measuring the system response to a series of test patterns comprised of sinusoidally alternating bars of maximum and minimum radiance at increasing spatial frequency, with the direction of the bars oriented perpendicular to the scan line for obtaining the response along the scan, and parallel to the scan lines for response normal to the scan. Square-wave test patterns can be used in lieu of sinusoidal patterns with no loss of accuracy for the higher spatial frequencies where only the fundamental of the square wave is passed by the optics and scanning aperture; the MTF is then equal to $\pi/4$ times the square wave response. Since the performance of the imaging system usually varies with temperature, the calibration should be repeated at several temperatures over the expected range. When the system configuration permits, it is desirable to include a provision for in-orbit verification of the radiometric calibration at several levels by viewing known radiance sources such as dark space, solar illuminated targets, and/or measured temperature sources.

Both the launch and space environment must be considered in planning the testing program to demonstrate that the electronic imaging system will survive the launch and operate for the required lifetime in space. To insure an adequate margin of safety in the mechanical design, it is recommended that a prototype or first flight model of the imaging system be subjected to vibration levels that are 150% of the expected launch loads. Similarly, thermal–vacuum testing should include exposure to temperatures that are 10K beyond the highest and lowest temperatures the system is expected to experience in the appropriate operating or standby mode. Particularly where novel mechanical, lubrication, or cooling techniques are used, adequate life tests in thermal vacuum should be run to demonstrate the validity of the design.

The cleanliness of the vacuum chamber should be given special attention to prevent contamination of bearings when the chamber is vented back and air passes into bearing assemblies enclosed within labyrinth seals. During the vacuum tests, optical elements, detectors, and radiator surfaces must be protected from evaporated lubricant, combustion products of spacecraft thruster engines, and outgassing contaminants. This protection of the optical surfaces must extend to all phases of assembly, test, and handling to prevent degradation of any optical element.

Finally, since mechanical and electrical components all have some life limitation, it is important that the testing program does not use up a significant fraction of the system life before the beginning of space operations. Depending on the number of individual electronic imaging systems of the given designs that are produced, it may be preferable to severely limit the testing of the flight article and obtain life and reliability statistics from a number of identical systems, as is done for many components in the manned space program. However, when the variability in performance from item to item is great, as with many detectors and image tubes, it is usually necessary to verify the performance of each flight article.

GLOSSARY

1. Definition of Terms

Beam landing. The approach of scanning electrons to the target in a television camera tube. The term is most frequently used in connection with low-velocity scanning and the inherent problem of producing an orthogonal approach in areas away from the center line of deflection, especially at the extremes of the raster.

Cassegrain.[1] The name broadly applied to a number of folded reflecting telescope designs where the folding occurs before the prime focus. Traditionally, the Cassegrain telescope consists of a parabolic primary mirror and hyperbolic secondary mirror.

Clamp. A keyed switching circuit used to establish a predetermined reference potential at a given point in another circuit for the duration of each keying pulse.

The switching elements are usually a diode pair (sometimes a bridge quad) connected in opposite polarity, and keyed by push-pull pulses obtained from a source independent (except in timing) of the clamped signal.

The term is sometimes loosely applied to a keyed single-diode circuit in which the keying is accomplished by the signal in the clamped circuit.

Contrast ratio. The ratio of the maximum to the minimum radiance values in an image or a portion thereof. Generally the entire area of the picture is implied, but smaller areas may be specified as in "detail contrast."

Cross flex pivot. A joint between two bodies permitting small relative torsional motion through flexure of the joint.

D (read dee-star).* A figure of merit for solid-state detectors, expressed as the normalized detectivity and calculated as $(A \cdot \Delta f)^{1/2}/NEP$, where A is the detector area, Δf is the bandwidth of the signal, and NEP is the noise equivalent power; units for D^* are thus cm $Hz^{1/2}/W$.

Dall-Kirkham.[1] A Cassegrain configuration having an elliptical primary mirror and spherical secondary mirror, and providing a simple design for on-axis applications.

Dielectric tape camera. An electronic imaging device which stores a charge pattern from a photoconductor on a dielectric tape by direct contact with the tape. The usual embodiment involves dielectric tape having extremely high insulating properties so that a charge pattern can be stored over a long period.

---

[1]A description of these optical systems may be found in *Applied Optics and Optical Engineering,* by R. Kingslake, Academic Press, New York, 1969.

Dynamic range. The ratio of the overload level of a system or device to its noise level usually expressed in decibels.

Electron multiplier. A structure within an electron tube which employs secondary electron emission from solids to produce current amplification. The usual embodiment involves several successive stages of secondary emitters or dynodes which yield high overall amplification with low noise.

Erasure. Removal of stored image information. The term is applied generally to removal of information stored on photo-surfaces in picture tubes, on dielectric tape, or on magnetic tape.

Frame (in television). A time interval of a set of signals which make up the complete data presentation of a given scene.

Field (in television). One of the two or more equal parts into which a frame is divided in interlaced scanning.

Field of view. The entire angular expanse visible through an optical instrument at a given time. In television, the full field of view is restricted to a maximum angle equal to the angle subtended at the rear nodal point by the diagonal of the raster area in the sensor. A lens is usually chosen to provide at least the minimum desired resolution at the extremes of the diagonal.

Field-sequential color. A color system in which the individual primary colors are associated with successive fields.

Gamma. The exponent of the power law that is used to approximate the curve of the output magnitude versus input magnitude over the region of interest. For quantitative evaluation it is customary to plot the log of the output magnitude (ordinate) versus the log of the input magnitude (abscissa), as measured from a point corresponding to some reference black level, and select a straight line which approximates this plot over the region of interest and take its slope. If the plot departs seriously from linearity, it cannot be adequately described by a single value of gamma. Even when the plot is reasonably linear, the procedure for determining the approximation should be described.

Geometric integrity (scanning linearity). Adherence of the movement of a scanning device to its theoretically correct constant velocity, measured in terms of deviation of the spot from the correct position, at a given instant, in percentage of picture height. Measurements are usually made in two independent dimensions designated "horizontal linearity" and "vertical linearity."

Image dissector tube (dissector tube). A camera tube (imaging tube) in which an electron image produced by a photoemitting surface is focused in the plane of a defining aperture and is scanned past that aperture.

Image orthicon. A camera tube (imaging tube) in which an electron image is produced by a photoemitting surface and focused on one side of a separate storage target that is scanned on its opposite side by an electron beam, usually of low-velocity electrons. The usual embodiment includes an electron multiplier, which provides low-noise amplification of the signal contained in the return beam.

Integration. On a storage target in a television imaging tube, the process of accumulating charges as a function of time and of illumination on the scene. There are storage targets in several types of sensors, such as the photoconductor in a vidicon or the dielectric target in a image orthicon, SIT, or SEC.

Lag (camera tubes). A persistence of the electrical-charge image. The terms "sticking" and "burn" are used in the same sense to describe persistence of greater duration; in the latter case, permanent or nearly permanent persistence.

Limiting horizontal resolution. In the direction of scan, the spatial frequency whose amplitude is just discernible above the noise level. In practice, the lowest discernible signal level is generally about 2% to 5% of maximum level.

Maksutov.[1] A telescope consisting of a spherical primary mirror preceded by a negative meniscus lens having spherical surfaces to cancel the spherical aberration of the primary.

Modulation transfer function (MTF). In an optical-electrical transducer, the characteristic that defines the ratio of the amplitude of the electrical output signal to the amplitude of the spatial sinusoid at the input, as a function of frequency.

Multispectral imaging. A process of electronic imaging in more than one spectral band, as in a color television camera.

NEP. Noise equivalent power of a detector. This quantity is measured as the incident rms power that will produce a signal voltage equal to the rms noise voltage of the detector. It is a function of spectral frequency, modulation frequency, and detector area.

Photocathode. An electrode used for obtaining photoelectric emission.

Photoconductor. A semiconducting material whose resistivity changes as a function of incident light flux.

Photomultiplier. A phototube (nonimaging photoelectric sensor) with one or more dynodes (secondary emitters) between the photocathode and the output electrode. The chain of dynodes in the usual photomultiplier provides high-gain, low-noise amplification. (See *Electron multiplier.*)

Porch, front or back. Intervals of constant signal level before or after the sync pulse. The preceding interval is called the "front porch" and the trailing interval the "back porch." It should be mentioned that the picture signal is never allowed to occur during these porch intervals. Usually the porch level is "black" (or, in broadcast television slightly "blacker-than-black"), and porch intervals may be used for clamping or other signal-processing functions.

---

[1]A description of these optical systems may be found in *Applied Optics and Optical Engineering,* by R. Kingslake, Academic Press, New York, 1969.

Resolution. The degree to which fineness of detail is distinguished or delineated.

Optical resolution is usually measured in line-pairs per millimeter at the focal plane. A line-pair is composed of one black bar and one white bar, adjacent and of equal width. Practical gratings include several line-pairs or alternate black and white bars of equal width. A range of values is usually embodied in a measuring chart containing several gratings of progressive fineness. The term spatial frequency is sometimes used to describe the number of line-pairs in a linear unit (e.g., in a millimeter).

In television, resolution is usually measured in terms of the number of television lines per picture-height. The number of television lines is the *total* number of alternate black and white bars or lines of equal width in the height of the pattern used for measurement. Practical measuring charts usually include "resolution wedges" composed of alternate black and white bars tapering in width, but of equal width at any point along the centerline of the wedge.

Return beam vidicon (RBV). A vidicon in which a signal plate is not used, but the signal is derived from the remainder of the scanning beam which returns to an electron multiplier where low-noise amplification is provided.

Ritchey-Chretien.[1] A Cassegrain configuration having zero coma. The primary is a slightly oblate spheroid and the convex secondary closely approximates an ellipsoid.

Scan conversion. A process of transforming television signals at one scanning rate to television signals at another scanning rate, or from one coding method to another. An example of the conversion of scanning rates is that of changing a 10-frame, 200-line, sequential-scan picture to broadcast rates at 30 frames, 525 lines interlaced. An example of the conversion of coding systems is that of changing a field-sequential color signal to simultaneous color standards.

Scan efficiency. The ratio of active scan time of the image plane to the total time per line or per frame.

SEC sensor. A secondary emission conduction imaging (camera) tube in which an electron image from a photocathode (corresponding to an optical image) is accelerated toward a porous-solid target with a high secondary emission ratio, resulting in an amplified (by the target gain or secondary emission ratio) charge pattern that is released from the target by a scanning electron beam.

Shading. Brightness and modulation gradients in the reproduced picture, not in the original scene, but caused by the imaging sensor.

---

[1]A description of these optical systems may be found in *Applied Optics and Optical Engineering,* by R. Kingslake, Academic Press, New York, 1969.

Undesired gradients of either brightness or modulation may exist alone or in combination. Amplitude of the undesired signal variation is measured as a percentage of the maximum black-to-white signal amplitude. The brightness gradient is sometimes called pedestal shading, and the modulation gradient is sometimes called signal shading.

Sensitivity (camera or sensor devices). The relation between signal output current from the device and the illuminance or irradiance on its faceplate. Measurements are usually given in terms of signal current per unit of illuminance or irradiance of specified type, e.g., nanoamperes per lumen (of tungsten light at 2854°K) or per watt per square meter (of irradiance over a given spectral interval).

A transfer characteristic plot is sometimes used to describe sensitivity, made on log-log paper with illuminance or irradiance as the abscissa and output current as the ordinate.

Storage. The act of storing information. In electronic image sensors, depending on the type, selective storage of charges occurs either electrostatically in the capacitance of a photoconductor or other target, or by trapping of carriers within the semiconductor.

Sync, sync signal, synchronizing signal. The signal employed for synchronizing of scanning. In television the sync signal is composed of pulses at rates related to the line and field (or frame) frequencies.

Vidicon. A camera tube (imaging sensor) in which a charge density pattern is formed by photoconduction and stored on that surface of the photoconductor which is scanned by an electron beam, usually of low-velocity electrons. (Signal currents are collected from a signal plate.)

Wynne-Rosin.[1] A catadioptic (containing both refracting and reflecting elements) adaptation of the Dall-Kirkham telescope. A doublet lens, with spherical surfaces and nearly zero power, between the secondary mirror and the focus provides good off-axis correction of aberrations.

2. Photometric and Radiometric Units

Engineering in the field of image sensing is complicated by the duality of units, metric and English, together with two basic modes of measurement based on radiometric and photometric units. The terms, symbols, and formulation used in photometry originally provided a reasonable set of units since the photographic processes relate to the portrayal of images as observed by the human eye adapted to bright illumination. As long as the sensing device approximates the spectral sensitivity of the human eye, valid results can be obtained; when the sensor response is limited to some portion of the visible region, or extends beyond to either the ultraviolet or infrared, radiometric terms must be used. Photometric measurements are based on a standard source of luminous flux, measured in lumens, which stimulates the human eye or some sensor with similar

[1]A description of these optical systems may be found in *Applied Optics and Optical Engineering*, by R. Kingslake, Academic Press, New York, 1969.

sensitivity. Radiometric measurements are based on a source of energy that emits radiant flux measured in watts. To relate these two systems of measurement, a factor called luminous efficiency is introduced as the ratio of the visual output of the source to the total radiant energy required to produce that output. Thus, if the source emits L lumens per unit area and W watts per unit area, the luminous efficiency K is L/W lumens per watt, where L and W are termed the luminous emittance and radiant emittance, respectively. When the ratio is taken at a particular wavelength, it is termed spectral luminous efficiency K_λ, and the function $K(\lambda)$ is called the Standard Luminosity Curve.

A physical model that illustrates the relations of the parameters of a source, its emitted flux, and the observed effect at a distance is shown in figure 7. The following table lists the corresponding terms for photometric and radiometric systems of reference. The terms are defined in Table V including numerical relationships between units.

Table V.—Photometric and Radiometric Units

Parameter	Radiometric			Photometric		
	Term	SI (MKS) unit	Symbol	Term	SI (MKS) unit	Symbol
Source energy	Radiant energy	J	U	Luminous energy	talbot	Q
Total power	Radiant flux	W	P	Luminous flux	lm	F
Surface power density of source	Radiant emittance	W/m^2	W	Luminous emittance	lm/m^2	L
Source intensity	Radiant intensity	W/sr	J	Luminous intensity	lm/sr	I
Source "brightness"	Radiance	$(W/sr)/m^2$	N	Luminance	$(lm/sr)/m^2$	B
Incident power density at receiver	Irradiance	W/m^2	H	Illuminance	lm/m^2	E

Candela (formerly candle). Luminous intensity in the direction normal to a surface 1/600,000 square meter when the surface is a blackbody at the freezing temperature of platinum, 2037°K, at atmospheric pressure, 101,325 N/m^2.

Foot-candle. English unit of illuminance given by the luminous flux per square foot at a distance of one foot from a source of one candela, equal to one lumen per square foot or 10.76 meter-candles.

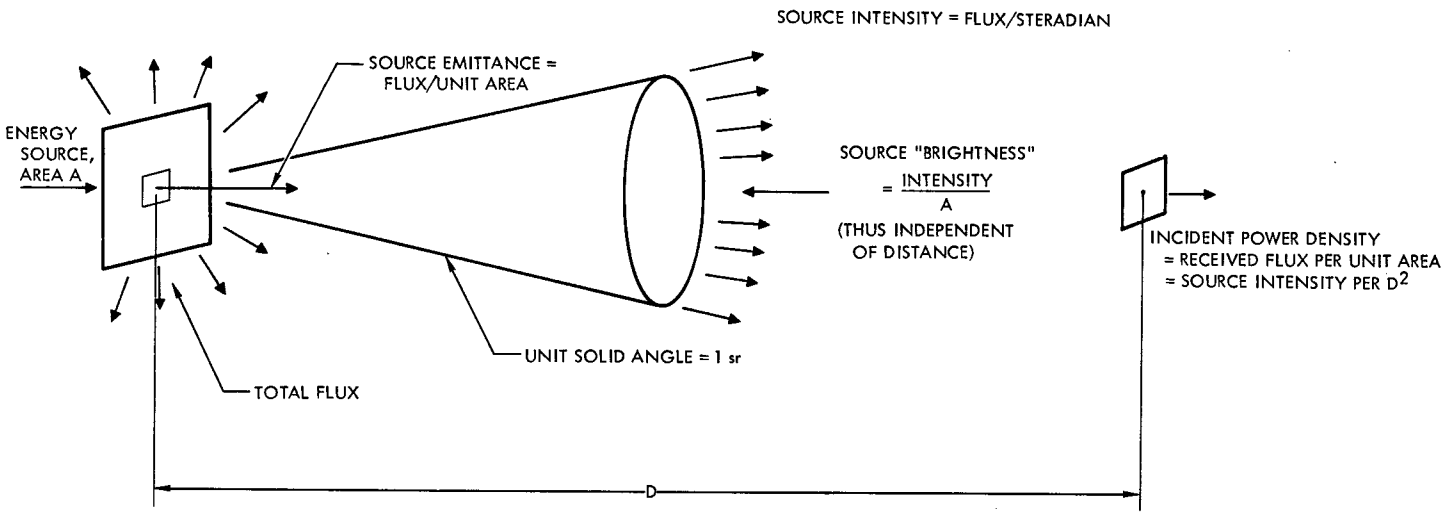

Figure 7.—Radiation model.

Foot-lambert. A unit of brightness, or luminance, of a Lambertian surface emitting one lumen per square foot; also the brightness of a Lambertian reflecting surface of reflectivity ρ illuminated by one $1/\rho$ foot-candles (Lambertian surfaces are perfectly diffuse surfaces with equal brightness or luminance from all directions). Numerically one foot-lambert equals $(1/\pi)$ (lm/sr)/ft^2 or 3.426 (lm/sr)/m^2.

Lumen. The luminous flux emitted within one unit solid angle (steradian) by a point source having a uniform intensity of one candela.

Lux. Unit of illuminance equal to one lumen per square meter.

Meter-candle. Unit of illuminance equal to one lumen per square meter or 0.0929 foot-candles.

Watt. One joule per second.

REFERENCES

1. Elle, B. L., et al., "The Lunar Orbiter Photographic System," *J. SMPTE,* Vol. 76, No. 8, Aug. 1967, pp. 733—773.

2. Goldberg, E. A., and Landon, V. D., "Key Equipment for TIROS I." *Astronautics,* June 1960.

3. Keigler, J. E., et al., "NIMBUS—An Advanced Meteorlogical Satellite," *RCA Engineer,* Vol. 9, No. 1, June–July 1963.

4. Ostrow, H., and Weinstein, O., *A Review of a Decade of Space Camera Systems Development for Meteorology.* SPIE 13th Annual Symposium, Redondo Beach, Calif., Aug. 1968.

5. Gravel, A. J., and Mesner, M. H., "The TV System for Ranger," *IEEE Trans. Broad.,* Vol. BC-11, No. 1, July 1965.

6. Freedman, L. A., "A Dielectric Tape Camera System for Meteorological Applications," *IEEE Trans. Aero. Electron. Sys.,* Vol. AES-2, No. 4, July 1966.

7. Anon., *Final Contract Report: Orbiting Astronomical Observatory Stellar TV Camera Subsystem,* RCA Contract Report No. PO H922 79C, Nov. 15, 1962.

8. Mesner, M. H., "The Television Camera System Used in Apollo 7 and 8 Command Modules," *J. SMPTE,* Vol. 79, No. 1, Jan. 1970.

9. Svenson, E. L., "The Lunar Television Camera," *Westinghouse Engineer,* Vol. 28, No. 2, March 1968.

10. Niemyer, L. L., Jr., "The Apollo Color Television Camera," *Westinghouse Engineer,* Vol. 29, No. 6, Nov. 1969.

11. Putterman, W., and Staniszewski, J., *RAE Antenna Aspect System.* Sixth Space Congress, Cocoa Beach, Fla.

12. Eastman, F. H., III, "A High Resolution Image Sensor," *J. SMPTE:* Vol. 79, No. 1, Jan. 1970.

13. Branchflower, G. A., and Koenig, E. W., *A Review of Image Dissector Meteorological Cameras and a View of Their Future,* Proceedings of the Sixth Space Congress, April 1969.

14. Schumacher, R. C., *Solar Flare Measurement Report,* Naval Research Laboratory, Space Sciences Division, June, 1970.

15. Heckel, D. T., "Unit and System Design of a Lunar Operating TV Camera," *J. SMPTE,* Vol. 76, No. 8, pp. 773–779.

16. Shaw, D. E., *Mariner Mars 1964 Project Report: Television Experiment, Part II-Rev. Picture Element Matrices,* Jet Propulsion Laboratory, Pasadena, Calif., March, 1968.

17. Anon., *Instrument Description for Mariner '69 Television,* Doc. 605-216, Jet Propulsion Laboratory, Pasadena, Calif., Aug. 1969; Also in *Applied Optics,* "Optics and the Mariner Imaging Instrument," D. R. Montgomery and L. A. Adams, Feb. 1970, Vol. 9, No. 2, pp. 277–287.

18. Anon., *Celescope Contract Final Report.* Contract NAS5–1535, 1968.

19. Anon., *Advanced Technology Satellite Design and Test Audit,* Doc. No. 66SD4495, Jet Propulsion Laboratory, Pasadena, Calif., Jan. 23, 1967 under Contract No. NAS5-9042.

20. Fischel, R., and Mobley, F., *Gravity Gradient Stabilization Studies with the Dodge Satellite,* Report TG-1112, Applied Physics Lab., Johns Hopkins University, Baltimore, Md., April 1970.

21. Anon., *Nimbus II User's Guide,* Prepared for Goddard Space Flight Center, under Contract NAS5-10114, July 1966.

22. Annable, R. V., "Radiant Cooling," *Appl. Optics,* Vol. 9, p. 197.

23. Thomsen, R. N., *ATS Spin-Scan Cloud Camera—Final Report,* Santa Barbara Research Center (University of Wisconsin Subcontract No. 1) June 1966.

24. Thomsen, R. N., *Multicolor Spin-Scan Cloud Camera*—Final Report, Santa Barbara Research Center (University of Wisconsin Subcontract No. 2) Dec. 1967.

25. Barncastle, L., *ITOS Scanning Radiometer—Final Report,* Santa Barbara Research Center (RCA Contract GF 42181-0201-F09) Dec. 1969.

26. Anon., *Nimbus IV Reference Manual,* GE Space Vehicles Div., Feb. 1970.

27. Lansing, J., and Norwood, V., *Final Report of Multispectral Point Scanner Study,* Hughes Aircraft Co. and Santa Barbara Research Center, under Contract NAS5-11624, 11647.

28. Anon., *Imaging Photopolarimeter Instrument Performance and Related Requirements,* Doc. PC-218.00, Ames Research Center, September 1969.

29. Anon., *Visible-Infrared Spin-Scan Radiometer for a Synchronous Meteorological Spacecraft.* Contract NAS 5-21139 Design Report, September 1970.

30. Aronson, A., *Application of Infrared Sensing in Meteorological Satellites.* Paper presented at North-East Electronic and Research Engineering Meeting, Boston, Mass., Nov. 6, 1970.

31. Tompkins, D. N., Final Technical Report, *Lunar Facsimile Capsule, Phase I Development,* Jet Propulsion Laboratory, Pasadena, Calif.

32. Anon., Philco-Ford Aeronautronics Div., Publication No. U2224, under JPL Contract 950462, Sept. 13, 1963.

33. Dishler, J., "Visual Sensor Systems in Space," *IEEE Trans. Commun. Tech.,* Vol. COM-15, Dec. 1967.

34. Anon., "Third Symposium on Photoelectronic Image Devices," *Advances in Electronics and Electron Physics,* Vols. 22A and 22B, Academic Press, New York, 1966.

35. Johnson, R. E., "Vidicon Performance Characteristics at Slow Scan Rates," *RCA Review,* March 1966.

36. Mesner, M. H., "Vidicon Applications for Spaceborne TV Cameras," *RCA Engineer,* Vol. 10, No. 2, Aug.—Sept. 1964.

37. Goetz, G. W., and Boerio, A. H., "Secondary Electron Conduction for Signal Amplification and Storage in Camera Tubes," *Proc. IEEE,* Vol. 52, Sept. 1964.

38. Schade, O. H., Sr., "The Resolving Power Functions and Quantum Processes of Television Cameras," *RCA Review,* Vol. 27, p. 460, Sept. 1967.

39. Blanchard, L. E., "Television Pictures of the Lunar Surface by Earthshine," *J. SMPTE,* Vol. 77, No. 4, April 1968, p. 351.

40. Saladi, I. T., and Schlesenger, F., "The FPS Vidicon," *Optical Spectra,* Feb. 1970, p. 53.

41. Heckel, D. T., et al., "Obtaining Color Television Pictures from Space," *J. SMPTE,* Vol. 77, No. 9, Sept. 1968, pp. 905–909.

42. Branchflower, G. A., and Koenig, E. W., "The Image Dissector, A New Approach to Spacecraft Sensors," *Proc. Fourth Space Congress,* Canaveral Council of Technical Societies, April 1967.

43. Morris, J. E., *Studies in the Degradation of the Five-Channel Radiometer,* NASA 66-14106, Sept. 1964.

44. *Handbook of Geophysics,* U.S. Air Force, Macmillan, N. Y., 1960.

45. Groggin, W. R., and Schroeder, J. B., "Beryllium Mirror Technology," *Proc. Electro-Optical Systems Design Conference,* New York, Sept. 1969.

46. Biberman, L. N., et al., *Low Light Level Devices.* IDA Report R-169, July 1970.

47. Anon., *High Voltage Breakdown Problems in Scientific Satellites,* Goddard Space Flight Center, Greenbelt, Md., Feb. 1966.

48. Holmes-Seidle, A. G., Leiderbach, F., and Poch, W. J., "The Prediction of Space Radiation Effects on Transistors and Solar Cells." *Conference Record,* IEEE Cat. F63, paper 22, May 1966.

49. Holmes-Seidle, A. G., and Poch, W. P., "The Design of a Weather Satellite for a Radiation Environment," paper presented at the *Symposium on Advances in Space Technology and Research,* British Interplanetary Society, Cambridge, England, Sept. 1970.

APPENDIX A

SIGNAL-TO-NOISE RATIO OF SENSORS

The signal-to-noise ratio of a television system is determined by the level of output signal and the summation of all of the system noise sources. The level of signal relates to luminous input and to the shape and slope of the transfer curve which may be expressed as sensor gamma. The noise is of two types: coherent noise and noncoherent noise. The coherent type is related to spatial parameters with pulses having a time relationship to the raster scanning (such as power supply spikes) or having a geometric relationship to the sensor retina (such as spots, smears, or granularity of the photosensitive surface). The noncoherent noise arises from a combination of the random nature of the photon emissions, beam bombardment, and thermal agitation in the input amplifier. Which of the noncoherent noise sources is of prime importance varies with the light levels being employed and the type of sensor.

In the case of the vidicon, the predominant noise is generated by the input amplifier and is determined by the noise factor of the amplifying device, the input resistance, the input capacitance, and the video bandwidth. The photon noise and the beam noise are usually comparatively small. In the case of the image orthicon, the preamplifier is the electron multiplier which has a very low noise factor. As a result, the shot noise from the scanning beam is predominant. The return-beam vidicon also falls into this category for the same reason. The very low light-level devices, such as the SIT sensor, the SEC vidicon, and the combination of sensors using intensifier input sections, are likely to have most of the noise generated by the action of photons on the photosensitive material.

The subjective effects of noise vary according to the source. Coherent noise, not being random as a function of time, presents patterns in the picture which become disturbing because of fixed positions and the ease of recognition on a display.

Noise from the preamplifier in a vidicon system is uniformly distributed through the gray scale range, being added to the signal from the sensor. Shot noise in an image orthicon has a somewhat different subjective effect, increasing with signal level. The effect is more pronounced in the case of photon-generated noise, where there is no noise in black areas and maximum noise in white areas. In fact, the picture may appear to be a geometric organization of noise which is intensity-modulated by picture information.

In a picture display, noise is a function of several factors including video bandwidth. In addition, the geometric dimensions of the noise pulses are determined by bandwidth, the noise having a coarser appearance for narrower bandwidths. However, a narrow-band system may be capable of higher gain ahead of the noise source, and this situation usually results in a better signal-to-noise ratio. Subjectively fine-grain noise is more acceptable than coarse noise and this negates some of the results anticipated from a purely mathematical viewpoint. For example, it does not suffice to attempt to improve the signal-to-noise ratio by deliberately reducing the passband, at a sacrifice of resolution, because of the unsatisfactory appearance of coarse noise.

The measurement of noise in a video system by classical techniques presents some problems because synchronizing and blanking pulses produce erroneous readings on noise meters. A technique which is widely used, even though it involves subjective interpretation, is to observe the relative heights of noise and video signal on an oscilloscope (A-scan). This kind of an observation in itself is a noise-averaging mechanism.

Signal-to-noise ratio is expressed as the ratio of low frequency, or dc, peak-to-peak signal (i.e., full scale white to black) to rms noise, and the value of rms noise is empirically determined to be 1/6 of the peak-to-peak noise observed on the oscilloscope. The expression for signal-to-noise ratio in decibels is:

$$SNR = 20 \log \frac{S_{p\text{-}p} \times 6}{N_{p\text{-}p}}$$

A signal-to-noise ratio of 35 to 50 dB is usually achieved in television studio practice.

A signal-to-noise ratio of 20 to 35 dB represents minimum performance in instrumentation television practice, and a ratio of 16 dB provides esthetically poor but recognizable patterns. At 10 dB, simple patterns may be crudely recognized.

The signal-to-noise ratio in the case of the standard vidicon is represented by the following formula:

$$SNR = \frac{I_s + I_d}{\left(4kTf\left[\frac{1}{R_i} + \frac{R_{eq}}{R_i^2} + \frac{4\pi^2 f^2 C_t^2 R_{eq}}{3} + 2e(\sigma + 1) I_{s+d}\right]\right)^{1/2}}$$

where

e = electron charge = 1.6×10^{-10} coulomb

σ = quantum gain = conduction electrons per photon

For most practical applications, only the first and third terms under the denominator radical are significant (ref. B-1).

k = Boltzmann's constant = 1.38×10^{-23} J/K

T = absolute temperature, Kelvin

f = upper limit of passband, hertz

C_i = input shunt capacitance

R_i = input load resistance

R_{eq} = equivalent noise resistance of preamplifier

I_s = signal current

I_d = vidicon dark current

$I_{s+d} = I_s + I_d$

q = charge on electron

The signal-to-noise ratio of an image orthicon is expressed as follows:

$$SNR = \frac{I_s}{\left(f\left[2\epsilon I K_m^2 + 4kT\left(\frac{1 + R_{eq}}{R_i} + \frac{4\pi^2 f^2 C_i^2 R_{eq}}{3} \right) \right] \right)^{1/2}}$$

where

I_s = signal current

f = upper limit of passband, hertz

ϵ = charge on the electron = 1.6×10^{-19} C

I = beam current

K_m = electron multiplier noise factor

k = Boltzmann's constant = 1.38×10^{-23} joules/Kelvin

R_1 = input load resistance

R_{eq} = noise equivalent resistance of input amplifier

T = temperature, K

C_1 = input shunt capacitance

The signal-to-noise ratio of an image dissector may be expressed as follows:

$$SNR = \frac{1}{K}\left(\frac{SE\frac{d}{M^2}}{2f\epsilon} \right)^{1/2}$$

where

K = noise contribution of multiplier—about 1.25

S = photocathode sensitivity, amperes/lumen

E = illumination on cathode, lumens/meter^2

d = scanning aperture area, meter^2

M = electron image magnification

f = upper limit of passband, hertz

ϵ = charge on the electron = 1.6×10^{-19} C

For detector noise, the frequency dependence of mean-square noise voltage in semiconductor infrared detectors has been found to follow the form

$$\left|N(f)\right|^2 = \left[\frac{K_1}{f^\alpha} + \frac{K_2}{1+\omega^2 t_d^2} + \frac{4kTR}{f}\right] \text{volts}^2$$

where

K_1, K_2 are proportionality factors

$\alpha \approx 1$

$\omega = 2\pi f$, radians sec^{-1}

k = Boltzmann's constant, 1.38×10^{-23} joules/Kelvin

t_d = detector time constant, sec

T = temperature, Kelvin

R = detector resistance, ohms

f = upper limit of passband, hertz

The first term is current, or "1/*f*," noise which predominates at low frequencies and is not well understood. The second term is generation-recombination (g-r) noise, which is the statistical fluctuation in the concentration of carriers in the detector and is dominant at intermediate frequencies. Thermal, or Johnson, noise becomes dominant at high frequencies and is due to the random motion of charge carriers.

REFERENCES

A-1. Dehaan, E. F., "Signal-to-Noise Ratio of Image Devices," *Advances in Electronics and Electron Physics,* Vol. XII, p. 291, Academic Press, New York, 1960.

APPENDIX B

DEFINITION AND DETERMINATION OF RESOLVING POWER

The resolution and gray scale performance of electronic imaging systems is readily available as shown in tables III and IV. However, since instrument designers usually reference these data to high-contrast, wide-dynamic-range, stationary targets, the true relationship of such performance data to the accomplishment of mission goals is more complex. For example, the object size that can be resolved is seldom given by the resolution value in table III converted to object space, nor correspondingly for scanners is it likely to be the instantaneous field of view of table IV times the object distance. The dependence of performance on several interrelated parameters requires analysis and engineering judgment to relate laboratory data to real scene conditions (refs. B-1 and B-2). Resolution values measured in the laboratory will, in practice, be a function of the scene luminance and contrast and of the signal-to-noise ratio realized in the system. Gray-step detection is also a function of luminance and noise as well as of sensor gamma. Both sensitivity and signal-to-noise ratio will depend upon the spectral range of the scene (ref. B-3). In addition to these factors, an even more difficult aspect is their subjective dependence on scene content, that is the complexity of the scene, the predominance of straight lines or arcs, the presence of recognizable patterns, and so on (ref. B-4).

A mathematical approach to these relationships can be derived from the basis of the MTF of the imaging system, the contrast and average luminance of the scene, and the resultant signal-to-noise ratio of the system (ref. B-5). To apply these relationships to a calculation of image system performance, a criterion is required for determining whether the signal corresponding to a given target is detectable. In practice, the criterion is related to a particular type of test target which has the primary virtue of analytical tractability; the size of this target is described in a reciprocal way by associating a spatial frequency with it. Usually referred to as the Tri-Bar or Air Force test chart, a portion of which is shown in figure B-1 along with the pertinent nomenclature, this type of reference scene provides sinusoidal modulation amenable to MTF analysis. A widely accepted criterion for limiting resolution requires 50% probability of detection of at least one of the tri-bars. Empirical results of controlled tests with photographic images containing known amounts of noise, as well as a statistical evaluation of the probability, show that this criterion corresponds to a 4 dB ratio of the peak-to-peak value of the signal from the tri-bar to the rms noise, measured electrically at the display when the detector scan is normal to the tri-bar pattern (refs. B-6 and B-7).

Figure B-1 shows that in addition to the spatial frequency, the two other identifying parameters of the scene are the average luminance and modulation. A family of curves can then be constructed of the modulation required for detection, or resolution, converting the values to spatial frequency and exposure at the image plane, as shown in figure B-2. These curves inherently include the effect of the sensor gamma since the ordinate is the modulation of the output signal while scanning the given target.

To determine the resolution actually achieved by the imaging system, a second family of curves is required, which presents the modulation output of the imaging system, again as a function of

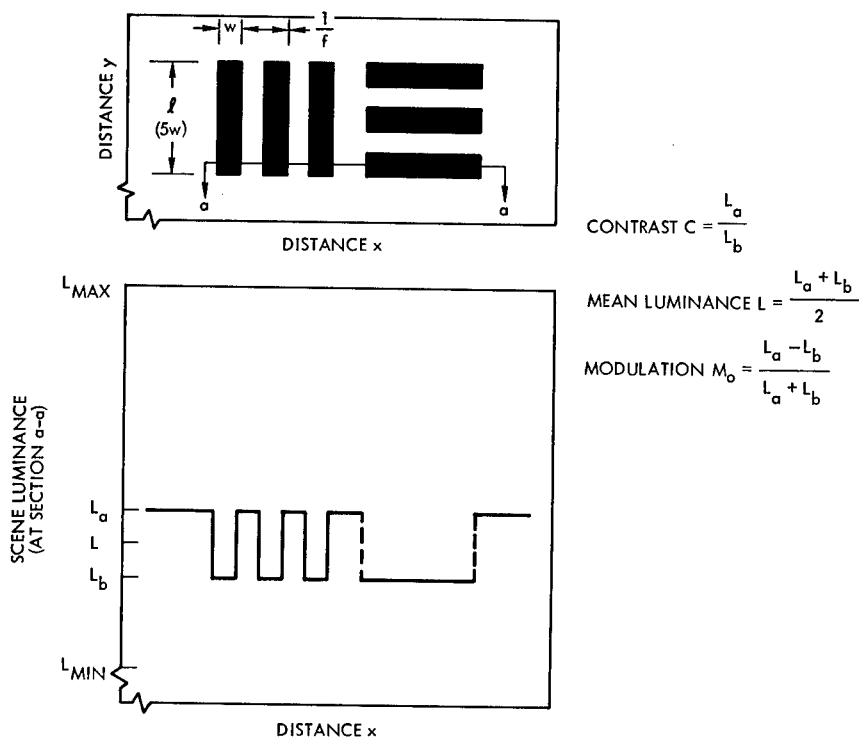

Figure B-1.—Target parameters.

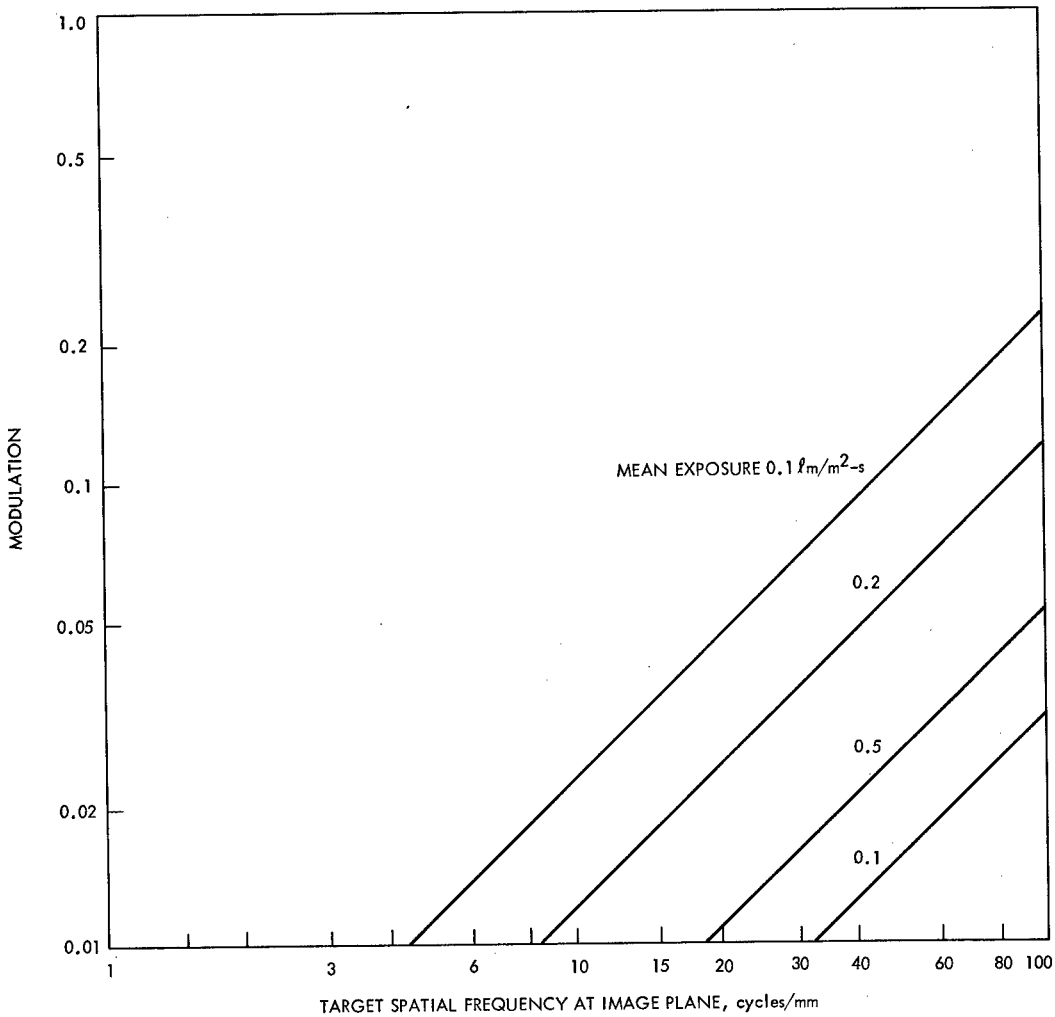

Figure B-2.—Detection thresholds.

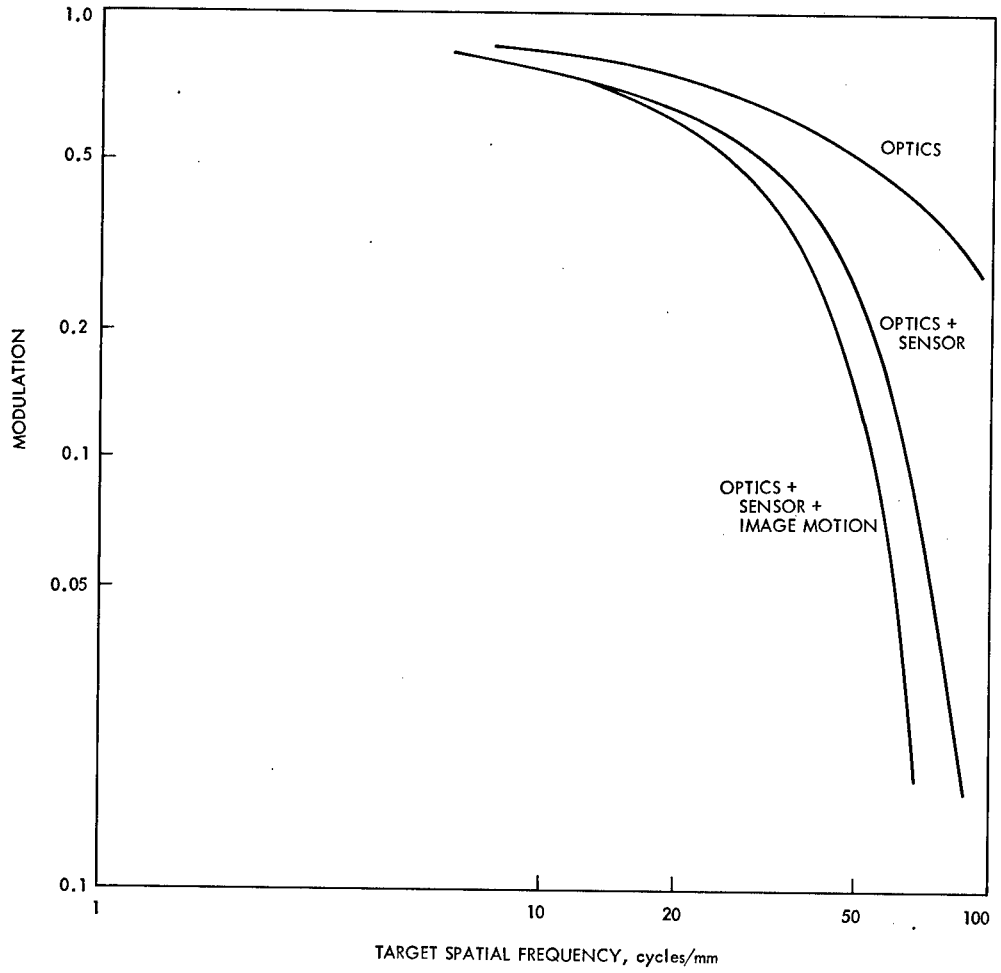

Figure B-3.—Modulation transfer function factors.

spatial frequency and target contrast. This modulation transfer function (MTF) for the system is the product of the MTFs of the component parts as shown in figure B-3, with the effect of image motion also expressed as an equivalent MTF. (The MTF is often presented on linear coordinates, giving the characteristic long "tail" in figure B-4, but the logarithmic frequency scale of figure B-3 is more amenable to the determination of resolution).

Finally, by repeating the system MTF for a set of scene contrasts and plotting on the same coordinates as the previous detectability curves, the actual resolution of the imaging system can be found as the spatial frequency at the intersection of the MTF of appropriate contrast with the detectability threshold of appropriate exposure. Figure B-5 illustrates these composite curves, showing indeed that higher exposure, giving greater signal (and hence greater signal-to-noise ratio) results in higher resolution, as does increased contrast for any fixed exposure. The object-space resolution is then obtained simply by geometry of object distance to focal length, so that for a particular application, the abscissa scale could be labeled in terms of the resolved object size. It should also be noted that the increased exposure at the image can be provided by any combination of increased scene luminance, increased exposure time, and increased optical gain

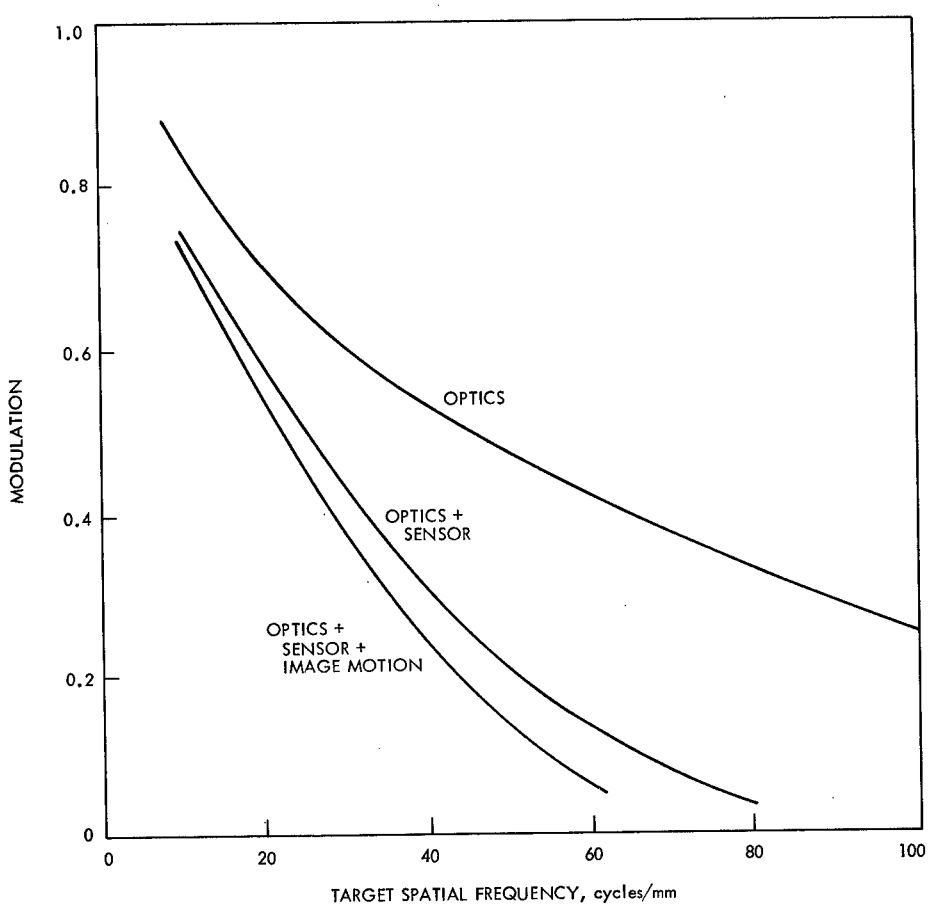

Figure B-4.—Modulation transfer function linear coordinates.

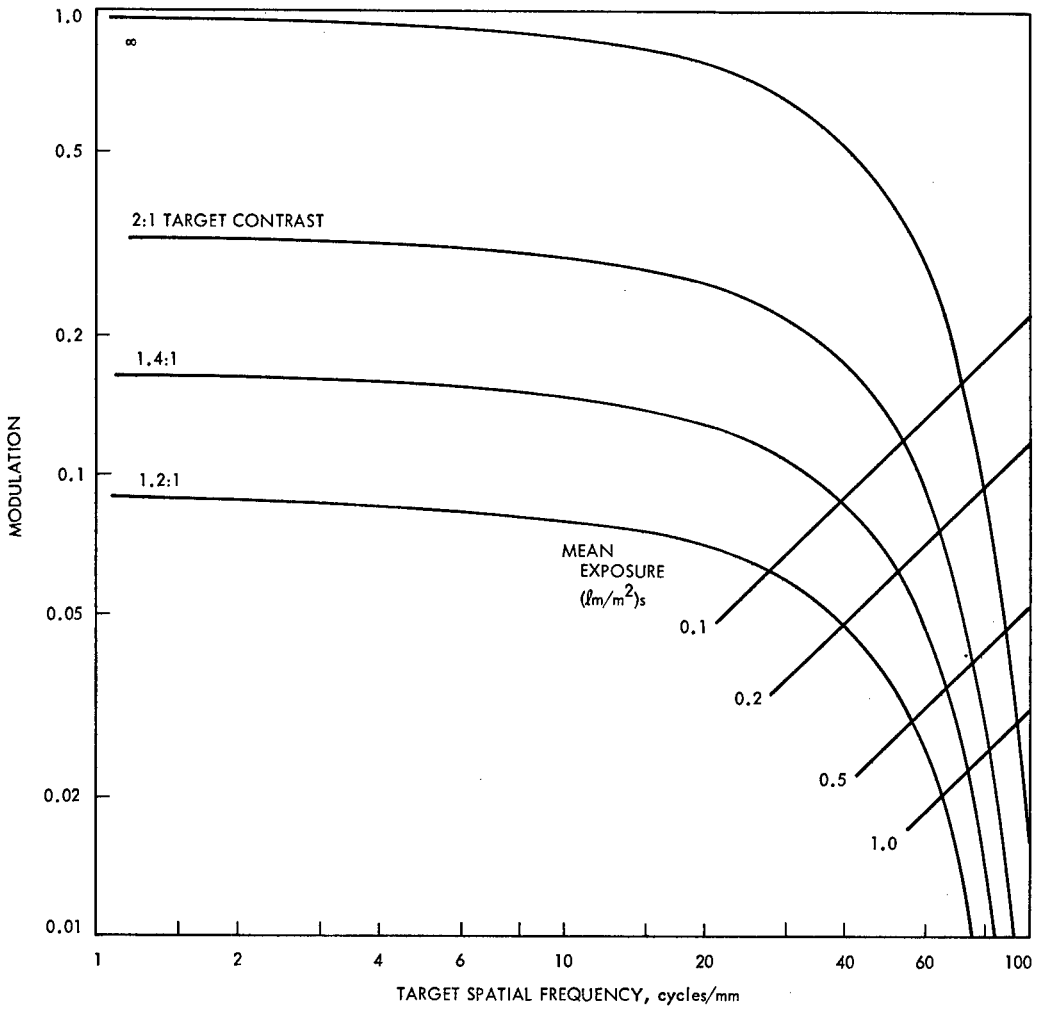

Figure B-5.—Resolving power curves.

(although faster optics will require an iteration of the MTF, as a larger aperture usually entails some decrease of MTF). Since many electronic imaging systems employ some form of high-frequency emphasis or aperture correction to enhance resolution, a refinement of the preceding curves is necessary in those cases. Figure B-6 shows the multiplication of the MTF by the aperture correction curve, to give a resultant extended MTF, and the correction of the threshold curve for the increased noise as well as signal at the high frequencies. Again the net system resolution is the intersection of these modified curves; of course, the full family would again be plotted for several values of target contrast and exposure.

The resolution performance as a function of exposure and contrast is frequently presented by interchanging the ordinate and the exposure parameter of the detection curve, plotting the locus of the intersection points. For any particular optical system and exposure time of a given imaging system, the exposure value can be converted to the corresponding irradiance onto the system. The resulting plots are referred to as areal image modulation (AIM) curves for that system, the name having originated in aerial reconnaissance applications as describing the areal image modulation characteristics. A typical set of such curves is presented in figure B-7.

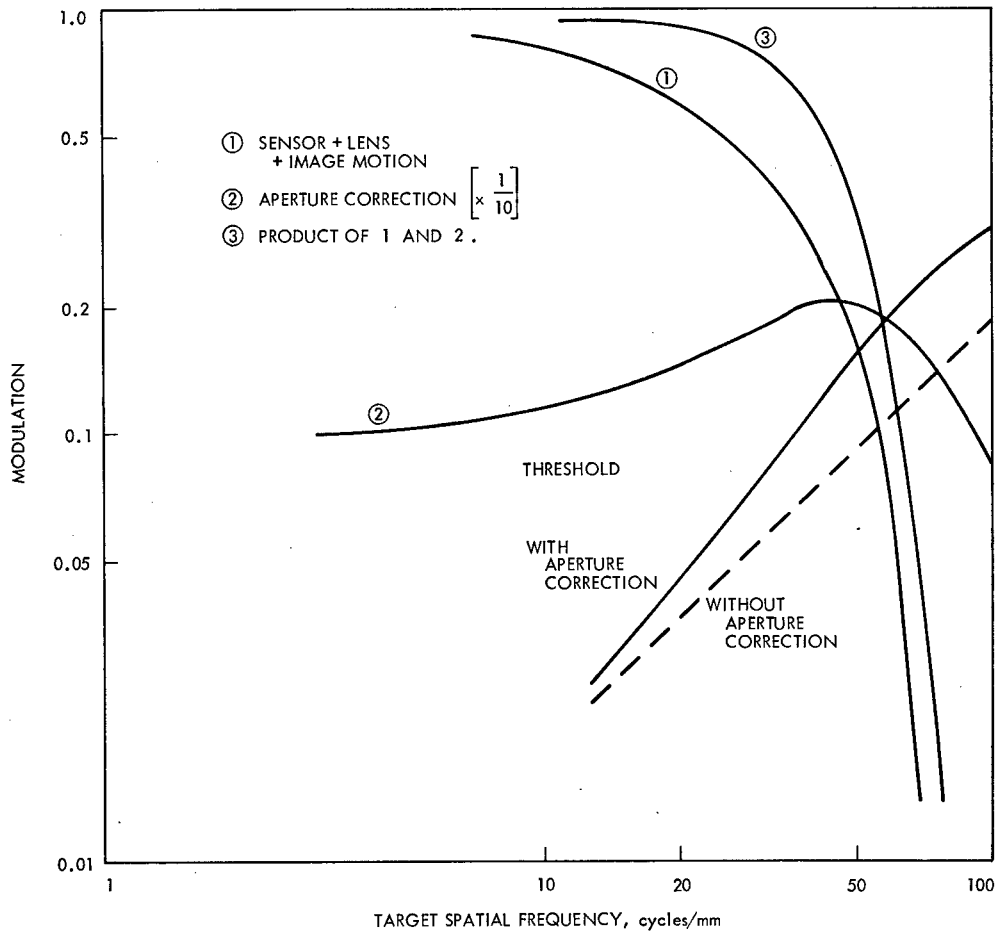

Figure B-6.—Aperture corrected resolving power.

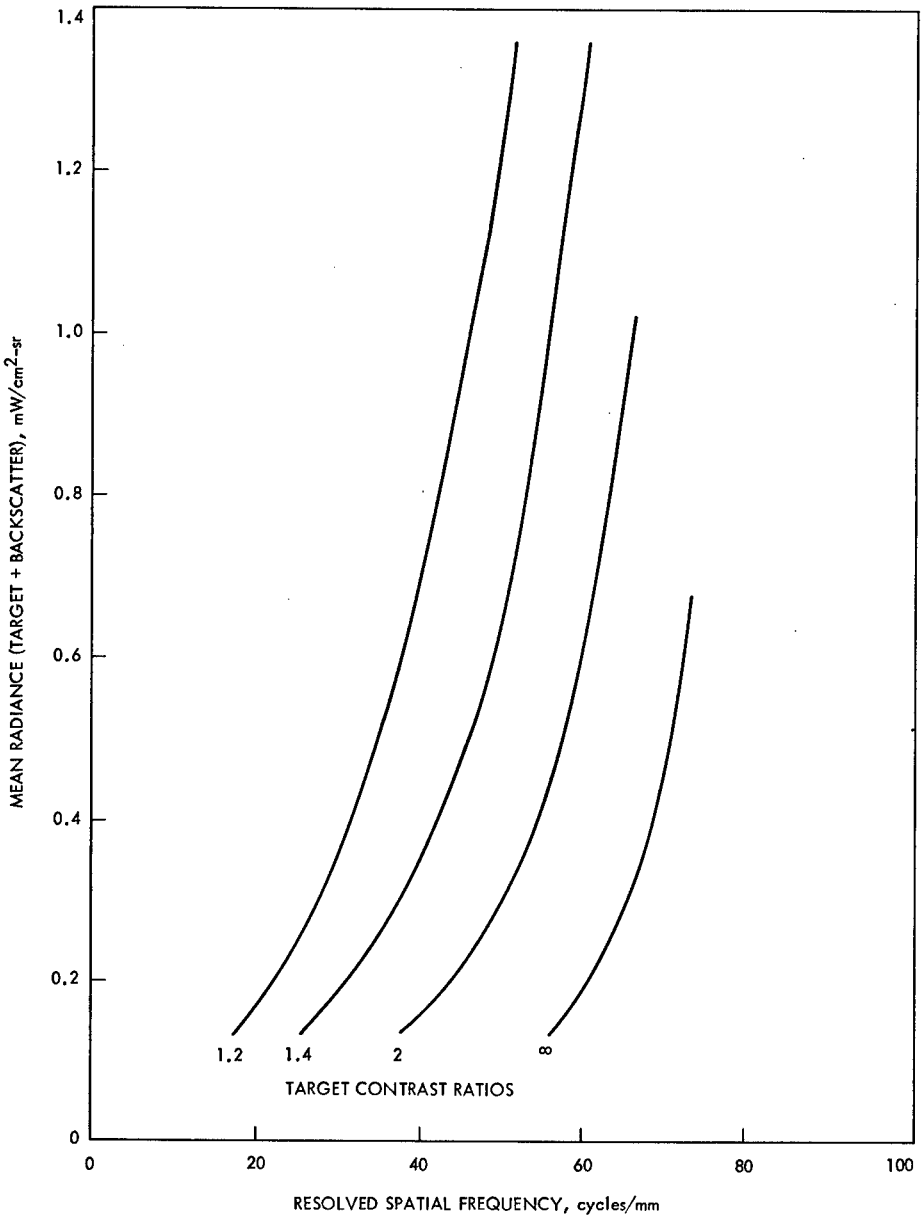

Figure B-7.—Typical areal image modulation characteristics curves.

Aliasing is a phenomenon that is analogous to signal distortion in electrically sampled data systems in which the Nyquist Criterion is violated. It results when the spatial sampling frequency of the line scan raster is less than twice the spatial frequency bandwidth of the scene information which is imaged. The following description is based on a facsimile camera; however, this phenomenon is also found in other line scan imaging systems.

The instantaneous field of view of the facsimile camera is determined by the photodetector pinhole aperture and distance from the objective lens. A mirror-scanning mechanism on the object side of the lens provides the vertical line scans, and an azimuth rotation of the line-scan assembly provides the spacing between successive lines. The shape of the pinhole aperture is generally designed to be circular, or is circular because either the photodetector itself or an optical fiber is used to define the aperture. The azimuth stepping interval between successive line scans is designed to be equal to the instantaneous field of view so that successive line scans are contiguous to each other. The facsimile camera design for Ranger is a typical example.

The facsimile camera MTF *along* the line scan is the product of the lens, pinhole, and sensor electronics MTFs; *normal* to the line scan, it is the product of only the lens and pinhole MTFs. If the electronics are designed to neither degrade nor enhance the MTF along the line scan, then the system MTFs parallel and normal to the line scan are determined only by the lens and pinhole. But, if we use a facsimile camera of this design to image, for example, the targets shown in figure B-8, then the images also shown in this figure can result. The extraneous patterns are the result of aliasing. If the target were to consist of more or less random patterns, as do most natural scenes, then the extraneous patterns will also be random and may be regarded as noise. This noise will, of course, also degrade image quality, but in a way which cannot be easily evaluated. The problem one is inevitably confronted with when evaluating the amount of image degradation due to aliasing is that it depends not only on the camera design but also on the spatial frequency distribution of the radiant energy reflected from the target. This leads to the conclusion that the specification of horizontal and vertical MTF alone is insufficient to adequately establish performance characteristics and, in fact, can lead to a system that severely distorts target information. The specification of normal to the line scan MTF must be supplemented by the careful specification of aperture shape and interval between successive lines.

SP-8051	Solid Rocket Motor Igniters, March 1971
SP-8053 (Structures)	Nuclear and Space Radiation Effects on Materials, June 1970
SP-8054 (Structures)	Space Radiation Protection, June 1970
SP-8055 (Structures)	Prevention of Coupled Structure-Propulsion Instability (Pogo), October 1970
SP-8056 (Structures)	Flight Separation Mechanisms, October 1970
SP-8057 (Structures)	Structural Design Criteria Applicable to a Space Shuttle, November 1970
SP-8058 (Guidance and Control)	Spacecraft Aerodynamic Torques, January 1971
SP-8059 (Guidance and Control)	Spacecraft Attitude Control During Thrusting Maneuvers, February 1971
SP-8060 (Structures)	Compartment Venting, November 1970
SP-8061 (Structures)	Interaction With Umbilicals and Launch Stand, August 1970
SP-8065 (Guidance and Control)	Tubular Spacecraft Booms (Extendible, Reel Stored), February 1971
SP-8070 (Guidance and Control)	Spaceborne Digital Computer Systems, March 1971
SP-8071 (Guidance and Control)	Passive Gravity-Gradient Libration Dampers, February 1971